sulting from exchange interactions between the $S_h = {}^1/_2$ ground state of the low-spin siroheme and the $S_c = {}^1/_2$ state of the cluster. This coupling is antiferromagnetic in the sense that the electron spins of the heme and the cluster are coupled antiparallel. However, since we do not know whether the cluster is attached at site I or site II to the siroheme, the sign of the factor $F_I$ is unknown and, thus, the sign of $k_{1h}$ is undetermined, as in $SiR^{2-}/(Gdm)_2SO_4$. By studying $SiR^{1-}$–$S^{2-}$ in a strong applied field we have determined that $J > 6$ cm$^{-1}$.

It is interesting to note that the signs of $J$ are different for $SiR^{2-}/(Gdm)_2SO_4$ and for $SiR^{1-}$–$S^{2-}$. Since $J = k_{1h}F_1$, both $k_{1h}$ and $F_1$ determine its sign. It is clear from the Mössbauer data that the iron–sulfur cluster is in the same state in both complexes. Therefore, we consider it unlikely that the link between the cluster and the siroheme has switched from a type I site to a type II site between the two complexes under discussion. This, then, suggests that the signs of $k_{1h}$ differ between the two complexes, i.e., the coupling is ferromagnetic in one complex and antiferromagnetic in the other. It is not surprising that the exchange interactions between the heme and the cluster are different in the two complexes because the low-spin ferric heme of $SiR^{1-}$–$S^{2-}$ has one unpaired d-electron whereas the high-spin ferrous iron of $SiR^{2-}/(Gdm)_2SO_4$ has four. Thus, the two complexes can develop quite different exchange pathways.

We have discussed in the Results section that the $g$ values of the "$g = 2.29$" species can be fitted with the model developed for $SiR^{2-}/(Gdm)_2SO_4$. Our present evidence suggests that the the siroheme of the "$g = 2.29$" species is not high-spin ferrous, although our data do not strictly rule out such an assignment. It appears that the siroheme of the "$g = 2.29$" species is in a state more closely related to that of $SiR^{1-}$ than that of the "$g_1 = 5$" species. The optical data, however, give quite a different picture. Janick and Siegel[8] have shown that the UV/vis spectra of the "$g = 2.29$" and the "$g_1 = 5$" species are virtually identical and quite distinct from that of $SiR^{1-}$. Since the optical spectra were recorded at room temperature and the EPR and Mössbauer data were obtained at temperatures below 200 K, the possibility of a spin transition of the siroheme iron has to be considered. Low-temperature optical studies are in preparation.

In conclusion, we have analyzed the EPR and Mössbauer data of $SiR^{2-}/(Gdm)_2SO_4$ and complexes with sulfide, and we have demonstrated exchange coupling between the siroheme and the iron–sulfur cluster. Thus far, we have provided evidence for exchange coupling in eight different states of SiR. In this study we have been able, for the first time, to determine the strength of the coupling. It is clear that the magnitude and signs of $J$ vary noticeably between the different states (see also ref 5), indicating that different exchange pathways are utilized. We have presented here and elsewhere models for the description of the exchange coupling which should provide a framework for further explorations of this unique arrangement of prosthetic groups.

**Acknowledgment.** This work was supported by NIH Grants GM-32210 (to L.M.S.) and GM-22701 (to E.M.), NSF Grant PCM-83-06964 (E.M.), and Veterans Administration Project Grant 7875-01 (to L.M.S.).

**Registry No.** NADPH-sulfite reductase, 9029-35-0; siroheme, 52553-42-1; sulfide, 18496-25-8.

# Metal Alkoxides—Models for Metal Oxides. 4.[1] Alkyne Adducts of Ditungsten Hexaalkoxides and Evidence for an Equilibrium between Dimetallatetrahedrane and Methylidynemetal Complexes: $W_2(\mu\text{-}C_2H_2) \rightleftharpoons 2W{\equiv}CH$

**Malcolm H. Chisholm,* Kirsten Folting, David M. Hoffman, and John C. Huffman**

*Contribution from the Department of Chemistry and Molecular Structure Center, Indiana University, Bloomington, Indiana 47405.* *Received January 24, 1984*

**Abstract:** In the presence of pyridine, alkyne adducts of ditungsten hexaalkoxides of formula $W_2(OR)_6(\mu\text{-}C_2R_2')(py)_n$, where R = *t*-Bu, R′ = H, and $n$ = 1, R = *i*-Pr, R′ = H, and $n$ = 2, and R = $CH_2$-*t*-Bu, R′ = Me, and $n$ = 2, have been isolated and characterized by variable-temperature NMR studies and single-crystal X-ray crystallography. In each compound there is a pseudotetrahedral $W_2(\mu\text{-}C_2)$ core with C–C distances (1.38–1.44 Å) and W–W distances (2.57–2.67 Å) that are approaching those of C–C and W–W single bonds. This implies a substantial rehybridization of triple bonds toward the idealized dimetallatetrahedrane in the reaction $(RO)_3W{\equiv}W(OR)_3 + R'C{\equiv}CR' \rightarrow (RO)_6W_2(C_2R'_2)$. Steric factors are important in controlling both the length of the W–W and C–C bonds of the central $W_2(\mu\text{-}C_2R'_2)$ moiety and the geometry about the tungsten atoms. Counting the $\mu\text{-}C_2R_2$ ligand to occupy one coordination site to each metal, the structure of the *tert*-butoxy compound is based on two fused trigonal-bipyramidal moieties sharing a common equatorial ($C_2R_2$) and axial (OR) edge; the neopentoxide has tungsten atoms that share an edge of a trigonal bipyramid and an octahedron and the isopropoxide has two octahedral tungsten atoms fused along a common face formed by two O-*i*-Pr ligands and the $\mu\text{-}C_2H_2$ ligand. All three compounds are fluxional on the NMR time scale though low-temperature limiting spectra consistent with expectations based on the structures found in the solid state are observed. Labeling studies, involving $H^{13}C^{13}CH$ and $D^{12}C^{12}CD$, suggest that the ethyne adduct $W_2(O\text{-}t\text{-}Bu)_6(\mu\text{-}C_2H_2)(py)$ is in equilibrium with $(t\text{-}BuO)_3W{\equiv}CH$. These studies are compared with related studies by Cotton and Schrock and their co-workers who have previously noted the formation of alkylidyne ligands in the reactions between $W_2(O\text{-}t\text{-}Bu)_6$ and disubstituted alkynes RC≡CR where R = alkyl and phenyl. (i) Crystal data for $W_2(O\text{-}t\text{-}Bu)_6(\mu\text{-}C_2H_2)(py)\cdot{}^1/_2py$ at −160 °C: $a$ = 17.399 (5) Å, $b$ = 11.336 (3) Å, $c$ = 11.216 (3) Å, $\alpha$ = 71.53 (1)°, $\beta$ = 113.72 (1)°, $\gamma$ = 98.90 (2)°, $Z$ = 2, $d_{calcd}$ = 1.714 g cm$^{-3}$, and space group $P\bar{1}$. (ii) Crystal data for $W_2(O\text{-}i\text{-}Pr)_6(py)_2(\mu\text{-}C_2H_2)$ at −165 °C: $a$ = 19.061 (11) Å, $b$ = 15.674 (7) Å, $c$ = 12.234 (5) Å, $\beta$ = 108.08 (1)°, $Z$ = 4, $d_{calcd}$ = 1.737 g cm$^{-3}$, and space group $P2_1/a$. (iii) Crystal data for $W_2(OCH_2\text{-}t\text{-}Bu)_6(\mu\text{-}C_2Me_2)(py)_2$: $a$ = 37.822 (21) Å, $b$ = 12.207 (5) Å, $c$ = 22.163 (9) Å, $\beta$ = 101.01 (2)°, $Z$ = 8, $d_{calcd}$ = 1.459 g cm$^{-3}$, and space group $C2/c$.

In this series of papers we are (i) examining structural and bonding relationships between metal oxides and metal alkoxides and (ii) investigating the chemistry of metal–carbon bonds supported by alkoxy ligands.[2] Previously, we reported[3] studies of

0002-7863/84/1506-6794$01.50/0 

the reactions between alkynes (HCCH, MeCCH, and MeCCMe) and hexaalkoxides of dimolybdenum, $Mo_2(OR)_6(M{\equiv}M)$, where R = *t*-Bu, *i*-Pr, and $CH_2$-*t*-Bu, and the isolation of pyridine adducts of type I and II. These were shown to be involved in the catalytic cyclotrimerization of alkynes to benzenes.

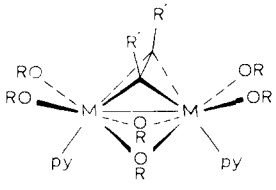

$Mo_2(OR)_6(py)_2(\mu\text{-}RCCR')$

R = *i*-Pr R' = H, Me

$R = CH_2$-*t*-Bu R' = H

I

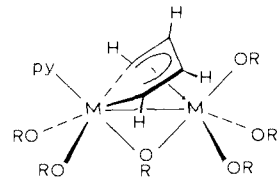

$Mo_2(OCH_2\text{-}t\text{-}Bu)_6(py)(\mu\text{-}C_4H_4)$

II

Recently, Schrock and co-workers[4] reported that $W_2(O\text{-}t\text{-}Bu)_6$[5,6] and alkynes react in hydrocarbon solvents at room temperature in a metathesis-like manner according to eq 1 and Cotton et al.[7]

$$W_2(O\text{-}t\text{-}Bu)_6 + RC{\equiv}CR \rightarrow 2(t\text{-}BuO)_3W{\equiv}CR \quad (1)$$

R = Me, Et, and Pr

found that at higher temperatures (ca. 70 °C) reaction between $W_2(O\text{-}t\text{-}Bu)_6$ and PhC≡CPh, in varying ratios, gave upon crystallization the compounds $(t\text{-}BuO)_2W(\mu\text{-}CPh)_2W(O\text{-}t\text{-}Bu)_2(M\text{–}M)$ and $(t\text{-}BuO)_2W(\mu\text{-}C_2Ph_2)_2W(O\text{-}t\text{-}Bu)_2$. In this paper we describe our preparation and characterization of alkyne adducts of hexaalkoxides of ditungsten. These are of particular interest in relationship to the observations of Schrock and Cotton and their co-workers and form interesting comparisons with alkyne adducts of more typical dinuclear organometallic species such as $Cp_2W_2(CO)_4(\mu\text{-}C_2H_2)$.[8] In a following paper,[9] we describe C–C coupling reactions involving these $W_2(\mu\text{-}C_2R_2)$ compounds in their reactions with alkynes and nitriles. A preliminary report of some of these findings has appeared.[10]

## Results and Discussion

**Syntheses and Physical Properties of $W_2(OR)_6(\mu\text{-}C_2R'_2)(py)_n$ Compounds.** The alkyne adducts of ditungsten hexaalkoxides have been prepared according to the general eq 2 (py = pyridine).

$$W_2(OR)_6 + 2py + R'C{\equiv}CR' \xrightarrow{\text{hexane}} W_2(OR)_6(\mu\text{-}C_2R'_2)(py)_n \quad (2)$$

R = *t*-Bu, R' = H, *n* = 1; R = *i*-Pr, R' = H, *n* = 2; R = $CH_2$-*t*-Bu, R' = Me, *n* = 2

The syntheses of the neopentoxy and isopropoxy compounds employ the pyridine adducts $W_2(OR)_6(py)_2$ as starting materials, whereas $W_2(O\text{-}t\text{-}Bu)_6$, free of pyridine ligation, is available.[6] In hexane solutions, there is rapid reversible binding of pyridine,

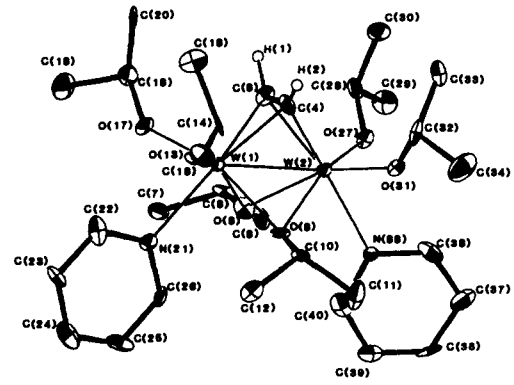

**Figure 1.** An ORTEP view of the $W_2(O\text{-}i\text{-}Pr)_6(py)_2(\mu\text{-}C_2H_2)$ molecule showing the atom number scheme used in the tables.

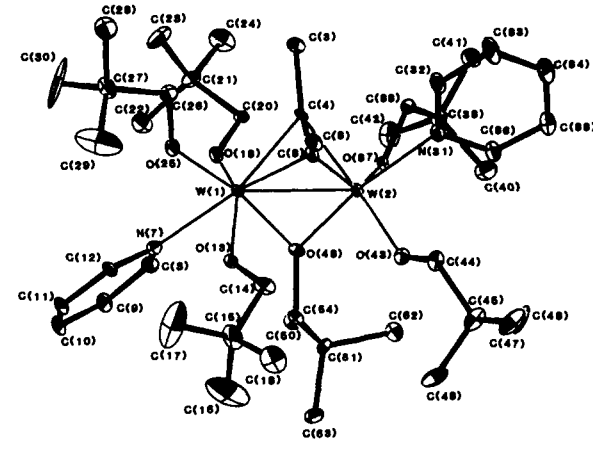

**Figure 2.** An ORTEP view of the $W_2(OCH_2\text{-}t\text{-}Bu)_6(py)_2(\mu\text{-}C_2Me_2)$ molecule showing the atom number scheme used in the tables.

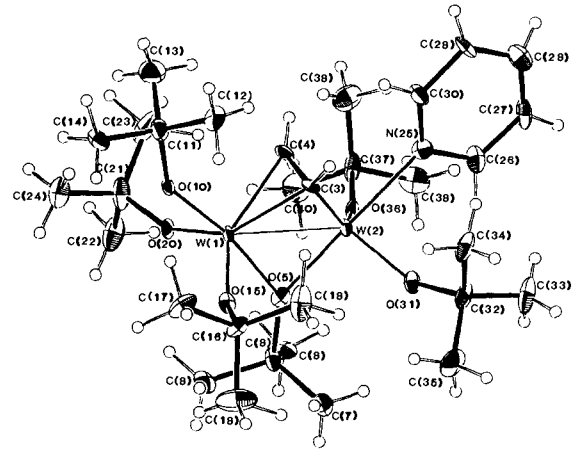

**Figure 3.** An ORTEP view of the $W_2(O\text{-}t\text{-}Bu)_6(py)(\mu\text{-}C_2H_2)$ molecule showing the atom number scheme used in the tables.

$W_2(OR)_6(py)_2 \rightleftharpoons W_2(OR)_6 + 2py$, and the position of equilibrium is sensitive to the steric properties of R. The presence of excess pyridine in reaction 2 is helpful in reducing the solubility of the alkyne adducts in the hexane solutions and thus assists in crystallization of the products. The preparation of the neopentoxy and isopropoxy compounds can be carried out at room temperature, but the *tert*-butoxy compound is best prepared below room temperature (ca. 0 °C) since it is thermally unstable. In all cases, care must be taken to add only 1 equiv of the alkyne since with excess alkyne further reactions occur yielding compounds containing the $W_2(\mu\text{-}C_4R_4)$ core.[9] Attempts to prepare a dimethylacetylene adduct of $W_2(O\text{-}t\text{-}Bu)_6$ failed: only the ethylidyne compound $[(t\text{-}BuO)_3W{\equiv}CMe]_2$ has been isolated from these reactions. Attempts to prepare $W_2(O\text{-}i\text{-}Pr)_6(\mu\text{-}C_2Me_2)(py)_2$ led to a mixture of products, including $W_2(\mu\text{-}C_4Me_4)$ containing

(1) Part 3. Chisholm, M. H.; Huffman, J. C.; Leonelli, J.; Rothwell, I. P. *J. Am. Chem. Soc.* **1982**, *104*, 7030.
(2) Chisholm, M. H. *ACS Symp. Ser.* **1983**, *No. 211*, 243.
(3) Chisholm, M. H.; Folting, K.; Huffman, J. C.; Rothwell, I. P. *J. Am. Chem. Soc.* **1982**, *104*, 4389.
(4) Shrock, R. R.; Listemann, M. L.; Sturgeoff, L. G. *J. Am. Chem. Soc.* **1982**, *104*, 4291.
(5) Chisholm, M. H.; Extine, M. W. *J. Am. Chem. Soc.* **1975**, *97*, 5625.
(6) Akiyama, M.; Chisholm, M. H.; Cotton, F. A.; Extine, M. W.; Haitko, D. A.; Little, D.; Fanwick, P. E. *Inorg. Chem.* **1979**, *18*, 2266.
(7) Cotton, F. A.; Schwotzer, W.; Shamshoum, E. S. *Organometallics* **1983**, *2*, 1167.
(8) Ginley, D. S.; Bock, C. R.; Wrighton, M. S.; Fischer, B.; Tipton, D. L.; Bau, R. *J. Organomet. Chem.* **1978**, *157*, 41.
(9) Chisholm, M. H.; Hoffman, D. M.; Huffman, J. C. *J. Am. Chem. Soc.*, following paper in this issue.
(10) Chisholm, M. H.; Folting, K.; Hoffman, D. M.; Huffman, J. C.; Leonelli, J. *J. Chem. Soc., Chem. Commun.* **1983**, 589.

**Table I.** Fractional Coordinates for the $W_2(O\text{-}i\text{-}Pr)_6(py)_2(C_2H_2)$ Molecule[a]

| atom | $10^4x$ | $10^4y$ | $10^4z$ | $10B_{iso}$, Å$^2$ |
|---|---|---|---|---|
| W(1) | 3261.6 (3) | 2266.8 (3) | 3167.1 (4) | 8 |
| W(2) | 3070.4 (3) | 3277.9 (3) | 1448.6 (4) | 9 |
| C(3) | 2754 (8) | 1974 (8) | 1421 (11) | 15 |
| C(4) | 2289 (7) | 2495 (9) | 1834 (11) | 15 |
| O(5) | 4102 (5) | 2649 (6) | 2413 (8) | 14 |
| C(6) | 4481 (7) | 2082 (9) | 1909 (11) | 14 |
| C(7) | 5036 (8) | 1559 (9) | 2853 (13) | 19 |
| C(8) | 4886 (7) | 2539 (9) | 1188 (12) | 15 |
| O(9) | 3426 (5) | 3605 (6) | 3201 (7) | 12 |
| C(10) | 3098 (7) | 4233 (8) | 3771 (10) | 11 |
| C(11) | 3235 (10) | 5131 (10) | 3377 (13) | 27 |
| C(12) | 3424 (8) | 4169 (9) | 5078 (11) | 17 |
| O(13) | 2702 (5) | 2300 (6) | 4251 (7) | 13 |
| C(14) | 1953 (7) | 2402 (8) | 4129 (10) | 15 |
| C(15) | 1536 (8) | 1566 (10) | 3815 (12) | 20 |
| C(16) | 1874 (8) | 2728 (11) | 5249 (2) | 21 |
| O(17) | 3481 (5) | 1072 (6) | 3452 (8) | 14 |
| C(18) | 3406 (8) | 312 (9) | 2774 (12) | 17 |
| C(19) | 3954 (9) | −323 (10) | 3498 (15) | 26 |
| C(20) | 2644 (8) | −26 (9) | 2488 (12) | 18 |
| N(21) | 4209 (6) | 2312 (7) | 4907 (9) | 12 |
| C(22) | 4139 (8) | 1791 (10) | 5743 (12) | 18 |
| C(23) | 4650 (7) | 1834 (9) | 6851 (11) | 15 |
| C(24) | 5239 (8) | 2419 (10) | 7079 (12) | 22 |
| C(25) | 5282 (7) | 2909 (9) | 6191 (12) | 18 |
| C(26) | 4762 (7) | 2858 (9) | 5106 (12) | 16 |
| O(27) | 3105 (5) | 3157 (5) | −111 (7) | 13 |
| C(28) | 3015 (8) | 2459 (9) | −890 (12) | 18 |
| C(29) | 3424 (8) | 2664 (11) | −1770 (12) | 23 |
| C(30) | 2212 (8) | 2287 (10) | −1486 (12) | 19 |
| O(31) | 2331 (5) | 4180 (6) | 1018 (8) | 14 |
| C(32) | 1564 (7) | 4238 (9) | 927 (11) | 13 |
| C(33) | 1107 (8) | 3857 (10) | −195 (12) | 20 |
| C(34) | 1383 (10) | 5170 (11) | 1037 (18) | 34 |
| N(35) | 3816 (6) | 4409 (7) | 1328 (9) | 12 |
| C(36) | 3571 (8) | 4972 (10) | 443 (12) | 21 |
| C(37) | 4002 (9) | 5644 (10) | 266 (14) | 24 |
| C(38) | 4724 (8) | 5705 (9) | 1046 (13) | 19 |
| C(39) | 4956 (8) | 5166 (10) | 1938 (13) | 20 |
| C(40) | 4514 (8) | 4506 (9) | 2059 (12) | 20 |

[a] Isotropic values are calculated by using the formula given by: Hamilton, W. C. *Acta Crystallogr.* **1959**, *12*, 609.

species, as deduced by $^1$H NMR spectroscopy. Presumably, here the C–C coupling reaction $W_2(\mu\text{-}C_2Me_2) + C_2Me_2 \rightarrow W_2(\mu\text{-}C_4Me_4)$ is kinetically competitive with the formation of the alkyne adduct in reaction 2. Clearly, the success of (2) depends upon a careful balance of steric factors that may alternatively favor alkylidyne formation or C–C coupling reactions.

The alkyne adducts are all air-sensitive materials but are stable in the crystalline state when stored in vacuo. The isopropoxy and neopentoxy compounds are stable in toluene-$d_8$ solutions in sealed NMR tubes for long periods (>1 week), but the *tert*-butoxy compound decomposes at room temperature over a period of 12 h. Analytical data, IR data, and $^1$H and $^{13}$C NMR data are given in the Experimental Section.

**Solid-State Structures.** Final atomic coordinates and isotropic thermal parameters are presented for $W_2(O\text{-}i\text{-}Pr)_6(py)_2(\mu\text{-}C_2H_2)$, $W_2(OCH_2\text{-}t\text{-}Bu)_6(py)_2(\mu\text{-}C_2Me_2)$, and $W_2(O\text{-}t\text{-}Bu)_6(py)(\mu\text{-}C_2H_2)\cdot{}^1/_2py$ in Tables I, II, and III, respectively; selected bond distances and angles are given in Tables IV, V, and VI, respectively, and ORTEP views of the three molecules are given in Figures 1, 2, and 3, respectively.

$W_2(O\text{-}i\text{-}Pr)_6(py)_2(\mu\text{-}C_2H_2)$ is isomorphous and isostructural with its molybdenum analogue.[3] The molecule has virtual $C_{2v}$ symmetry, and each tungsten atom achieves a pseudooctahedral coordination if the $\mu\text{-}C_2H_2$ ligand is considered as one ligand site and the W–W bond is ignored. The two octahedral units are joined in a confacial manner by a pair of O-*i*-Pr ligands (O(5) and O(9)) and the $\mu\text{-}C_2H_2$ ligand. The M–M distances 2.554 (1) (M = Mo) and 2.567 (1) Å (M = W) are virtually identical and the C–C distances of the $\mu\text{-}C_2H_2$ ligand, 1.368 (6) (M = Mo) and 1.394 (19) Å (M = W), and all other metal-ligand distances are equivalent to within $3\sigma$.

**Table II.** Fractional Coordinates for the $W_2(OCH_2\text{-}t\text{-}Bu)_6(py)_2(C_2Me_2)$ Molecule

| atom | $10^4x$ | $10^4y$ | $10^4z$ | $10B_{iso}$, Å$^2$ |
|---|---|---|---|---|
| W(1) | 1103.3 (1) | 1373.7 (4) | 8910.6 (2) | 12 |
| W(2) | 1353.1 (1) | 2427.7 (4) | 8061.2 (2) | 13 |
| C(3) | 1134 (3) | −216 (10) | 7671 (5) | 25 |
| C(4) | 1118 (3) | 874 (9) | 7977 (4) | 15 |
| C(5) | 862 (3) | 1683 (10) | 7927 (5) | 17 |
| C(6) | 474 (4) | 1719 (11) | 7597 (5) | 28 |
| N(7) | 1204 (3) | 1340 (8) | 9977 (4) | 22 |
| C(8) | 1538 (3) | 1389 (10) | 10312 (5) | 25 |
| C(9) | 1609 (4) | 1465 (11) | 10941 (5) | 32 |
| C(10) | 1322 (4) | 1493 (12) | 11256 (6) | 40 |
| C(11) | 977 (4) | 1387 (12) | 10907 (6) | 37 |
| C(12) | 928 (3) | 1343 (10) | 10277 (5) | 22 |
| O(13) | 780 (2) | 2514 (6) | 9128 (3) | 18 |
| C(14) | 553 (3) | 3314 (11) | 8828 (6) | 30 |
| C(15) | 324 (4) | 3870 (14) | 9215 (7) | 45 |
| C(16) | 594 (7) | 4500 (23) | 9728 (11) | 111 |
| C(17) | 122 (7) | 3186 (21) | 9520 (15) | 123 |
| C(18) | 86 (4) | 4712 (15) | 8837 (8) | 53 |
| O(19) | 1522 (2) | 432 (6) | 9166 (3) | 21 |
| C(20) | 1819 (3) | −22 (9) | 8948 (5) | 18 |
| C(21) | 1928 (3) | −1135 (10) | 9242 (6) | 25 |
| C(22) | 2022 (4) | −1015 (12) | 9947 (6) | 34 |
| C(23) | 1605 (4) | −1920 (12) | 9089 (7) | 45 |
| C(24) | 2243 (4) | −1551 (14) | 8990 (7) | 48 |
| O(25) | 757 (2) | 246 (7) | 8998 (3) | 22 |
| C(26) | 542 (4) | −488 (11) | 8606 (6) | 32 |
| C(27) | 276 (3) | −1065 (12) | 8915 (6) | 32 |
| C(28) | 48 (4) | −1851 (14) | 8471 (7) | 43 |
| C(29) | 36 (5) | −226 (24) | 9112 (13) | 111 |
| C(30) | 475 (8) | −1718 (24) | 9438 (11) | 143 |
| N(31) | 1280 (3) | 2430 (8) | 7033 (5) | 25 |
| C(32) | 1072 (4) | 1792 (12) | 6632 (6) | 33 |
| C(33) | 1059 (6) | 1855 (17) | 6006 (6) | 63 |
| C(34) | 1260 (6) | 2593 (16) | 5781 (7) | 66 |
| C(35) | 1489 (5) | 3283 (13) | 6194 (7) | 45 |
| C(36) | 1489 (4) | 3159 (12) | 6799 (6) | 31 |
| O(37) | 1846 (2) | 2060 (6) | 8022 (3) | 13 |
| C(38) | 2014 (3) | 1394 (10) | 7621 (5) | 22 |
| C(39) | 2421 (3) | 1670 (10) | 7688 (6) | 28 |
| C(40) | 2464 (4) | 2905 (12) | 7595 (7) | 39 |
| C(41) | 2558 (4) | 1048 (11) | 7186 (7) | 34 |
| C(42) | 2619 (3) | 1349 (13) | 8320 (7) | 39 |
| O(43) | 1188 (2) | 3954 (7) | 7936 (4) | 22 |
| C(44) | 921 (3) | 4481 (10) | 7501 (5) | 22 |
| C(45) | 985 (3) | 5704 (11) | 7522 (7) | 33 |
| C(46) | 964 (4) | 6174 (11) | 8154 (8) | 42 |
| C(47) | 1347 (4) | 5988 (12) | 7373 (8) | 41 |
| C(48) | 690 (4) | 6251 (12) | 7033 (8) | 48 |
| O(49) | 1488 (2) | 2656 (6) | 8982 (3) | 17 |
| C(50) | 1493 (3) | 3646 (9) | 9344 (5) | 17 |
| C(51) | 1867 (3) | 4174 (9) | 9501 (5) | 18 |
| C(52) | 1973 (3) | 4617 (11) | 8910 (6) | 26 |
| C(53) | 1835 (3) | 5114 (10) | 9932 (6) | 28 |
| C(54) | 2150 (3) | 3355 (11) | 9800 (6) | 29 |

The molecule is sterically congested, which probably accounts for the long W–N distances, 2.31 (1) Å (averaged) and the lability of the pyridine ligands toward dissociation in solution. A molecular model reveals that the $\mu\text{-}C_2H_2$ ligand is nestled in a pocket formed by the methyne protons of the six O-*i*-Pr ligands. The six methyne C–H bonds are all directed toward the $\mu\text{-}C_2H_2$ ligand, which leads one to suspect that, on steric grounds, it would be impossible to fit together a structurally related molecule in which *t*-Bu groups replace *i*-Pr groups. Similarly, replacing the $\mu\text{-}C_2H_2$ ligand by $\mu\text{-}C_2R_2$, where R = alkyl, would be expected to introduce internal steric congestion.

The neopentoxy dimethylacetylene complex $W_2(OCH_2\text{-}t\text{-}Bu)_6(py)_2(\mu\text{-}C_2Me_2)$, while having a similar formula to that of the isopropoxide, has a different structure having only a virtual mirror plane passing through the two tungsten atoms and bisecting the bridging $\mu\text{-}C_2Me_2$ ligand. There is only one bridging OR ligand that leads to two different tungsten atoms. Again counting

**Table III.** Fractional Coordinates for the $W_2(O\text{-}t\text{-}Bu)_6(py)(C_2H_2)\cdot{}^1/_2py$ Molecule

| atom | $10^4x$ | $10^4y$ | $10^4z$ | $10B_{iso}$, Å$^2$ |
|---|---|---|---|---|
| W(1) | 2255.3 (2) | 1881.8 (3) | 3973.1 (4) | 8 |
| W(2) | 2949.3 (2) | 1740.5 (3) | 6607.2 (4) | 9 |
| C(3) | 1763 (6) | 1094 (10) | 5512 (10) | 16 |
| C(4) | 1787 (6) | 2434 (9) | 5161 (9) | 12 |
| O(5) | 3501 (4) | 1821 (6) | 5326 (6) | 11 |
| C(6) | 4349 (6) | 1826 (9) | 5344 (10) | 14 |
| C(7) | 4718 (6) | 577 (10) | 6298 (10) | 19 |
| C(8) | 4845 (6) | 2902 (10) | 5842 (11) | 19 |
| C(9) | 4251 (6) | 1985 (10) | 3888 (10) | 19 |
| O(10) | 1165 (4) | 1949 (6) | 2471 (6) | 10 |
| C(11) | 277 (6) | 1935 (10) | 2093 (10) | 18 |
| C(12) | −18 (6) | 879 (11) | 3052 (11) | 24 |
| C(13) | 17 (7) | 3163 (11) | 2077 (12) | 27 |
| C(14) | −122 (6) | 1761 (11) | 681 (10) | 19 |
| O(15) | 2450 (4) | 354 (6) | 3741 (6) | 12 |
| C(16) | 2227 (6) | −899 (8) | 3726 (10) | 14 |
| C(17) | 1492 (6) | −959 (9) | 2389 (11) | 20 |
| C(18) | 1999 (8) | −1581 (11) | 4922 (11) | 31 |
| C(19) | 2990 (7) | −1437 (11) | 3774 (15) | 33 |
| O(20) | 2553 (4) | 3495 (5) | 2992 (6) | 12 |
| C(21) | 2345 (7) | 4752 (10) | 2150 (10) | 22 |
| C(22) | 3197 (7) | 5403 (10) | 2264 (11) | 27 |
| C(23) | 1892 (8) | 5353 (11) | 2690 (12) | 31 |
| C(24) | 1849 (7) | 4700 (10) | 714 (1) | 25 |
| N(25) | 2375 (5) | 1690 (7) | 8114 (8) | 15 |
| C(26) | 2918 (7) | 1710 (10) | 9366 (10) | 19 |
| C(27) | 2658 (17) | 1795 (10) | 10358 (10) | 21 |
| C(28) | 1822 (7) | 1778 (10) | 10095 (11) | 22 |
| C(29) | 1250 (6) | 1732 (9) | 8818 (10) | 17 |
| C(30) | 1563 (6) | 1684 (10) | 7870 (10) | 17 |
| O(31) | 3440 (4) | 204 (6) | 7877 (6) | 13 |
| C(32) | 3390 (6) | −1008 (9) | 8781 (10) | 19 |
| C(33) | 3874 (7) | −958 (11) | 10241 (11) | 27 |
| C(34) | 2492 (6) | −1419 (10) | 8561 (10) | 22 |
| C(35) | 3819 (8) | −1886 (10) | 8493 (12) | 27 |
| O(36) | 3504 (4) | 3214 (6) | 7086 (6) | 12 |
| C(37) | 3512 (7) | 4404 (9) | 7277 (10) | 18 |
| C(38) | 4126 (7) | 4364 (10) | 8723 (12) | 24 |
| C(39) | 2657 (7) | 4770 (10) | 7043 (12) | 26 |
| C(40) | 3862 (7) | 5348 (10) | 6296 (12) | 27 |
| C(41) | 490 (8) | 5872 (12) | 5604 (15) | 38 |
| C(42) | −168 (8) | 3824 (12) | 5781 (14) | 34 |
| C(43) | 340 (9) | 4702 (12) | 6396 (15) | 41 |

the $\mu$-$C_2R_2$ ligand to occupy only one coordination site and ignoring the M–M bond, one tungsten atom, W(1), is in a distorted octahedral environment being coordinated to three terminal OR ligands (O(13), O(19), and O(25)), pyridine (N(7)), a bridging OR ligand (O(49)), and the bridging alkyne (CTR). The terminal alkoxides O(13) and O(19) are bent away from the bridging alkyne so that the CTR–W(1)–O(19) and CTR–W(1)–O(13) angles deviate from 90° (105° and 106°). Presumably, this bending back of the terminal alkoxides is for steric reasons. The other tungsten atom, W(2), is in a pseudo-trigonal-bipyramidal environment consisting of two terminal alkoxides (O(43) and O(37)), the bridging alkoxide (O(49)), pyridine (N(31)), and the bridging 2-butyne ligand. The center of the C–C bond of the alkyne ligand and the two terminal $OCH_2$-*t*-Bu ligands occupy the three positions of the trigonal plane.

Molecules of $W_2(O\text{-}t\text{-}Bu)_6(py)(\mu\text{-}C_2H_2)$ have yet another geometry in the solid state, namely, that based on two fused trigonal bipyramids sharing a common equatorial site ($\mu$-$C_2H_2$) and an axial site ($\mu$-O-*t*-Bu). For each tungsten atom, the terminal alkoxy groups occupy sites within the trigonal plane but, for W(1), there is a terminal O-*t*-Bu ligand in an axial site (trans to the $\mu$-O-*t*-Bu ligand) while, for W(2), there is an axial pyridine ligand. Assuming the $\mu$-$C_2H_2$ ligand to be equivalent to a monodentate ligand represented by the midpoint of the C–C bond, CTR, the angles subtended at trigonal bipyramidally coordinated tungsten atoms are summarized in Table VII. Virtually all the angles fall within ±5° of the idealized 120°, 90°, and 180° required for equatorial–equatorial, axial–equatorial, and axial–axial bond angles, respectively.

Three further general points are worthy of note. (1) The W–W distances fall within a range that has previously been seen for W–W double and single bond distances supported by alkoxide ligands.[11] Cf. the W=W bond distances 2.499 (3) Å in the confacial bioctahedral compound $W_2(O\text{-}i\text{-}Pr)_6(py)_2(\mu\text{-}CO)$[1] and 2.483 (1) Å in the edge-shared octahedral compound $W_2Cl_4(OEt)_4(HOEt)_2$[12] and the W–W single bond distance of 2.715 (1) Å in $W_2Cl_4(OEt)_6$.[13] Also, there is a significant lengthening of the W–W distances as trigonal bipyramidal (tbp) tungsten atoms are substituted for octahedral (oct) tungsten atoms: $d$(W–W) = 2.567 (oct–oct), 2.602 (oct–tbp), and 2.665 Å (tbp–tbp). (2) The three alkyne complexes reported here have relatively long C–C(alkyne) distances compared to other dinuclear transition-metal complexes in which an alkyne ligand is bonded perpendicular to the M–M vector.[14] These typically have C–C distances of 1.34 (2) Å[14] comparable to that in ethylene, 1.337 (3) Å.[15] The $\mu$(C–C) distance, 1.44 Å, in $W_2(O\text{-}t\text{-}Bu)_6(py)(\mu\text{-}C_2H_2)$ may be compared with that claimed[16] for the longest C–C(alkyne) distance, 1.412 (17) Å, in a perpendicular alkyne $M_2$ complex, $Ir_2(CO)_4(PPh_3)_2(\mu\text{-}C_2HPh)$. (3) The W–OR distances for the terminal OR groups are notably shorter than those associated with bridging W–OR ligands, as is typically found, and fall in the range where some RO-to-W $\pi$ bonding is generally implicated.[11] Asymmetries are seen in the W–OR distances of the bridging OR ligands in $W_2(OCH_2\text{-}t\text{-}Bu)_6(py)_2(\mu\text{-}C_2Me_2)$ and $W_2(O\text{-}t\text{-}Bu)_6(py)(\mu\text{-}C_2H_2)$ reflecting, at least in part, the different trans influences of the OR and py ligands. A similar asymmetry is seen in the W–C distances of the $W_2(\mu\text{-}C_2)$ moiety in $W_2(OCH_2\text{-}t\text{-}Bu)_6(py)_2(\mu\text{-}C_2Me_2)$ where the alkyne group appears bound more strongly to the tbp tungsten atom. Other apparent asymmetries in the $W_2(\mu\text{-}C_2R_2)$ units such as the slight skew found for R = Me are not considered chemically significant since they fall within the 3$\sigma$ range of idealized positions.

**Bonding Considerations.** If the alkyne ligands were merely considered as four-electron donors, donating a pair of electrons to each metal atom, then the $W_2(\mu\text{-}C_2R_2)$ compounds reported here could be viewed as $d^3$–$d^3$ dimers with the potential of realizing a W–W triple bond. However, the relatively long W–W and C–C distances suggest that this would be an inappropriate view. An alternate limiting bonding description could be based on counting the bridging alkyne as a $\mu$-$C_2R_2^{4-}$ ligand spanning a $(W\text{-}W)^{10+}$ center. In this description, extensive W-to-$C_2R_2$ $\pi^*$ bonding results in limiting W–W and C–C single bonds: formation of a dimetallatetrahedrane. It is also necessary to allow for RO-to-W $\pi$ bonding that will mix in with metal–alkyne and metal–metal bonding. It is thus not possible to present a simple picture of the bonding in these molecules, and the observed trend in $d$(W-W) (oct–oct > oct–tbp > tbp–tbp) warrents the attention of a theoretical study. It should be noted, however, that the W–W and C–C distances in $W_2(O\text{-}t\text{-}Bu)_6(py)(\mu\text{-}C_2H_2)$ represents the closest approach to the limiting dimetallatetrahedrane thus far seen in organometallic chemistry.

**$^1$H NMR Studies.** The $^1$H NMR spectra of the alkyne adducts, in toluene-$d_8$ as a solvent, have been obtained at 360 MHz at various temperatures. The spectrum of $W_2(OCH_2\text{-}t\text{-}Bu)_6(py)_2(\mu\text{-}C_2Me_2)$ at +21 °C is consistent with that expected based upon the structure shown in Figure 2. Specifically, there are four *tert*-butyl signals in the ratio 2:2:1:1, and the methylene protons appear as two AB quartets (4 H:4 H) and two singlets (2 H:2 H), characteristic of neopentoxy groups that are respectively out of and contained in the molecular plane of symmetry. Upon

(11) For a general review of M–M and M–O distances in alkoxides of Mo and W, see: Chisholm, M. H. *Polyhedron* **1983**, *2*, 681.
(12) Anderson, L. B.; Cotton, F. A.; DeMarco, D.; Fang, A.; Isley, W. H.; Kolthammer, B. W. S.; Walton, R. A. *J. Am. Chem. Soc.* **1981**, *103*, 5078.
(13) Cotton, F. A.; DeMarco, D.; Kolthammer, B. W. S.; Walton, R. A. *Inorg. Chem.* **1981**, *20*, 3048.
(14) For a listing of C–C distances in perpendicular $M_2(\mu\text{-}C_2R_2)$ complexes, see: Hoffman, D. M.; Hoffmann, R.; Fisel, C. R. *J. Am. Chem. Soc.* **1982**, *104*, 3858.
(15) Kutchitsu, K. *J. Chem. Phys.* **1966**, *44*, 906.
(16) Angoletta, M.; Bellon, P. L.; DeMartin, F.; Sansoni, M. *J. Organomet. Chem.* **1981**, *208*, C12.

**Table IV.** Selected Bond Distances (Å) and Bond Angles (deg) for the $W_2(O\text{-}i\text{-}Pr)_6(py)_2(\mu\text{-}C_2H_2)$ Molecule

| A | B | dist | A | B | dist |
|---|---|---|---|---|---|
| W(1) | W(2) | 2.567 (1) | W(2) | O(5) | 2.183 (9) |
| W(1) | O(5) | 2.175 (8) | W(2) | O(9) | 2.099 (8) |
| W(1) | O(9) | 2.114 (9) | W(2) | O(27) | 1.940 (8) |
| W(1) | O(13) | 1.948 (8) | W(2) | O(31) | 1.950 (9) |
| W(1) | O(17) | 1.927 (9) | W(2) | N(35) | 2.306 (10) |
| W(1) | N(21) | 2.318 (11) | W(2) | C(3) | 2.118 (13) |
| W(1) | C(3) | 2.096 (14) | W(2) | C(4) | 2.094 (14) |
| W(1) | C(4) | 2.080 (13) | C(3) | C(4) | 1.394 (19) |

| A | B | C | angle | A | B | C | angle |
|---|---|---|---|---|---|---|---|
| W(2) | W(1) | O(5) | 54.0 (2) | O(5) | W(2) | O(27) | 101.0 (4) |
| W(2) | W(1) | O(9) | 52.2 (2) | O(5) | W(2) | O(31) | 157.4 (4) |
| W(2) | W(1) | O(13) | 125.1 (3) | O(5) | W(2) | N(35) | 84.5 (4) |
| W(2) | W(1) | O(17) | 135.7 (3) | O(5) | W(2) | C(3) | 77.6 (4) |
| W(2) | W(1) | N(21) | 127.1 (3) | O(5) | W(2) | C(4) | 101.6 (4) |
| W(2) | W(1) | C(3) | 52.9 (4) | O(9) | W(2) | O(27) | 158.5 (4) |
| W(2) | W(1) | C(4) | 52.3 (4) | O(9) | W(2) | O(31) | 94.5 (4) |
| O(5) | W(1) | O(9) | 66.6 (3) | O(9) | W(2) | N(35) | 82.4 (3) |
| O(5) | W(1) | O(13) | 156.3 (4) | O(9) | W(2) | C(3) | 104.2 (4) |
| O(5) | W(1) | O(17) | 101.7 (4) | O(9) | W(2) | C(4) | 86.5 (4) |
| O(5) | W(1) | N(21) | 85.2 (4) | O(27) | W(2) | O(31) | 92.5 (4) |
| O(5) | W(1) | C(3) | 78.2 (4) | O(27) | W(2) | N(35) | 78.7 (4) |
| O(5) | W(1) | C(4) | 102.3 (4) | O(27) | W(2) | C(3) | 89.4 (4) |
| O(9) | W(1) | O(13) | 94.0 (4) | O(27) | W(2) | C(4) | 113.9 (4) |
| O(9) | W(1) | O(17) | 159.3 (3) | O(31) | W(2) | N(35) | 80.4 (4) |
| O(9) | W(1) | N(21) | 83.3 (4) | O(31) | W(2) | C(3) | 121.0 (5) |
| O(9) | W(1) | C(3) | 104.5 (4) | O(31) | W(2) | C(4) | 89.2 (5) |
| O(9) | W(1) | C(4) | 86.5 (4) | N(35) | W(2) | C(3) | 156.2 (5) |
| O(13) | W(1) | O(17) | 92.2 (4) | N(35) | W(2) | C(4) | 164.1 (5) |
| O(13) | W(1) | N(21) | 78.8 (4) | C(3) | W(2) | C(4) | 38.7 (5) |
| O(13) | W(1) | C(3) | 121.6 (4) | W(1) | O(5) | W(2) | 72.2 (3) |
| O(13) | W(1) | C(4) | 89.4 (5) | W(1) | O(5) | C(6) | 122.9 (8) |
| O(17) | W(1) | N(21) | 78.5 (4) | W(2) | O(5) | C(6) | 123.3 (8) |
| O(17) | W(1) | C(3) | 88.9 (5) | W(1) | O(9) | W(2) | 75.1 (3) |
| O(17) | W(1) | C(4) | 113.4 (5) | W(1) | O(9) | C(10) | 126.6 (7) |
| N(21) | W(1) | C(3) | 156.7 (5) | W(2) | O(9) | C(10) | 126.9 (7) |
| N(21) | W(1) | C(4) | 163.8 (5) | W(1) | O(13) | C(14) | 133.2 (7) |
| C(3) | W(1) | C(4) | 39.0 (5) | W(1) | O(17) | C(18) | 136.6 (8) |
| W(1) | W(2) | O(5) | 53.8 (2) | W(2) | O(27) | C(28) | 134.3 (8) |
| W(1) | W(2) | O(9) | 52.7 (2) | W(2) | O(31) | C(32) | 134.4 (8) |
| W(1) | W(2) | O(27) | 135.0 (3) | W(1) | C(3) | W(2) | 75.1 (4) |
| W(1) | W(2) | O(31) | 125.2 (3) | W(1) | C(3) | C(4) | 69.9 (8) |
| W(1) | W(2) | N(35) | 126.4 (3) | W(2) | C(3) | C(4) | 69.8 (8) |
| W(1) | W(2) | C(3) | 52.1 (4) | W(1) | C(4) | W(2) | 75.9 (5) |
| W(1) | W(2) | C(4) | 51.8 (3) | W(1) | C(4) | C(3) | 71.1 (8) |
| O(5) | W(2) | O(9) | 66.7 (3) | W(2) | C(4) | C(3) | 71.6 (8) |

raising the temperature, the neopentoxy signals broaden and at +80 °C are approaching coalescence. No significant decomposition occurred at +80 °C in the NMR probe over a period of ca. 1 h.

By contrast, the $W_2(O\text{-}i\text{-}Pr)_6(py)_2(\mu\text{-}C_2H_2)$ molecule is fluxional on the $^1H$ NMR time scale at +21 °C, showing only broad resonances for both the methyl and methyne protons of the O-*i*-Pr ligands. Upon lowering the temperature, a limiting spectrum is obtained at −20 °C that is consistent with expectations based on the molecular structure found in the solid state and is analogous to that previously described in detail for $Mo_2(O\text{-}i\text{-}Pr)_6(py)_2(\mu\text{-}C_2H_2)$.[3] The addition of pyridine-$d_5$ (40 equiv/$W_2$ complex) did not significantly change the spectra above −20 °C. The insensitivity of the rate of alkoxy group site exchange toward pyridine concentration suggests an intramolecular mechanism of scrambling that does not require py dissociation. An attractive mechanism for O-*i*-Pr site exchange involves the opening and closing of O-*i*-Pr bridges whereby the structure of $W_2(O\text{-}i\text{-}Pr)_6(py)_2(\mu\text{-}C_2H_2)$ found in the solid state, having two O-*i*-Pr bridges, is in rapid equilibrium with a structure akin to that found for $W_2(OCH_2\text{-}t\text{-}Bu)_6(py)_2(\mu\text{-}C_2Me_2)$, having only one OR bridge. The "relative" rigidity of the $\mu\text{-}C_2Me_2$ compound can be understood to result from the alkyne methyl substituents that disfavor the facile formation of the dibridged $(\mu\text{-}OR)_2$ structure. At temperatures above +20 °C, pyridine dissociation from $W_2(O\text{-}i\text{-}Pr)_6(py)_2(\mu\text{-}C_2H_2)$ becomes rapid and reversible on the NMR time scale, leading to time-averaged signals in the presence of added pyridine. Similarly, for $W_2(OCH_2\text{-}t\text{-}Bu)_6(py)_2(\mu\text{-}C_2Me_2)$ at +80 °C, reversible pyridine dissociation becomes rapid on the NMR time scale.

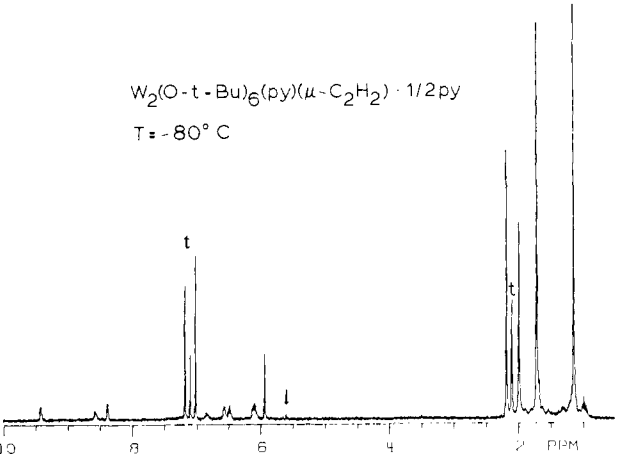


**Figure 4.** $^1H$ NMR spectrum of a crystalline sample of $W_2(O\text{-}t\text{-}Bu)_6(py)(\mu\text{-}C_2H_2)\cdot{}^1/_2py$ dissolved in toluene-$d_8$ recorded at 360 MHz and at −80 °C. The signals denoted by "t" arise from the protio impurities in the solvent. The signal due to the $\mu\text{-}C_2H_2$ ligand is at $\delta$ 5.92 and that due to the W≡CH group is indicated by the arrow at $\delta$ 5.47.

The spectra associated with $W_2(O\text{-}t\text{-}Bu)_6(py)(\mu\text{-}C_2H_2)\cdot{}^1/_2py$ are also temperature dependent. At +21 °C, there is one sharp

**Table V.** Selected Bond Distances (Å) and Angles (deg) for the $W_2(OCH_2\text{-}t\text{-}Bu)_6(py)_2(\mu\text{-}C_2Me_2)$ Molecule

| A | B | dist | A | B | dist |
|---|---|---|---|---|---|
| W(1) | W(2) | 2.602 (1) | W(2) | O(37) | 1.937 (7) |
| W(1) | O(13) | 1.973 (7) | W(2) | O(43) | 1.968 (8) |
| W(1) | O(19) | 1.952 (8) | W(2) | O(49) | 2.025 (7) |
| W(1) | O(25) | 1.936 (7) | W(2) | N(31) | 2.243 (10) |
| W(1) | O(49) | 2.123 (7) | W(2) | C(4) | 2.088 (11) |
| W(1) | N(7) | 2.322 (9) | W(2) | C(5) | 2.039 (11) |
| W(1) | C(4) | 2.168 (10) | C(4) | C(5) | 1.374 (15) |
| W(1) | C(5) | 2.229 (10) | | | |

| A | B | C | angle | A | B | C | angle |
|---|---|---|---|---|---|---|---|
| W(2) | W(1) | O(13) | 99.0 (2) | O(37) | W(2) | O(49) | 91.0 (3) |
| W(2) | W(1) | O(19) | 96.5 (2) | O(37) | W(2) | N(31) | 83.6 (3) |
| W(2) | W(1) | O(25) | 140.4 (2) | O(37) | W(2) | C(4) | 100.5 (4) |
| W(2) | W(1) | O(49) | 49.5 (2) | O(37) | W(2) | C(5) | 138.5 (4) |
| W(2) | W(1) | N(7) | 137.2 (2) | O(43) | W(2) | O(49) | 91.4 (3) |
| W(2) | W(1) | C(4) | 50.9 (3) | O(43) | W(2) | N(31) | 83.2 (3) |
| W(2) | W(1) | C(5) | 49.2 (3) | O(43) | W(2) | C(4) | 136.8 (4) |
| O(13) | W(1) | O(19) | 148.4 (3) | O(43) | W(2) | C(5) | 98.3 (4) |
| O(13) | W(1) | O(25) | 90.8 (3) | O(49) | W(2) | N(31) | 169.1 (3) |
| O(13) | W(1) | O(49) | 84.8 (3) | O(49) | W(2) | C(4) | 103.6 (3) |
| O(13) | W(1) | N(7) | 75.7 (3) | O(49) | W(2) | C(5) | 104.8 (4) |
| O(13) | W(1) | C(4) | 124.2 (4) | N(31) | W(2) | C(4) | 86.7 (4) |
| O(13) | W(1) | C(5) | 87.8 (4) | N(31) | W(2) | C(5) | 85.4 (4) |
| O(19) | W(1) | O(25) | 94.6 (3) | C(4) | W(2) | C(5) | 38.9 (4) |
| O(19) | W(1) | O(49) | 84.6 (3) | W(1) | O(13) | C(14) | 137.4 (7) |
| O(19) | W(1) | N(7) | 74.2 (3) | W(1) | O(19) | C(20) | 141.6 (7) |
| O(19) | W(1) | C(4) | 86.8 (4) | W(1) | O(25) | C(26) | 136.0 (7) |
| O(19) | W(1) | C(5) | 122.8 (4) | W(2) | O(37) | C(38) | 134.5 (7) |
| O(25) | W(1) | O(49) | 170.0 (3) | W(2) | O(43) | C(44) | 134.0 (7) |
| O(25) | W(1) | N(7) | 82.5 (3) | W(1) | O(49) | W(2) | 77.7 (2) |
| O(25) | W(1) | C(4) | 92.1 (4) | W(1) | O(49) | C(50) | 126.3 (6) |
| O(25) | W(1) | C(5) | 93.4 (4) | W(2) | O(49) | C(50) | 130.3 (6) |
| O(49) | W(1) | N(7) | 87.7 (3) | W(1) | C(4) | W(2) | 75.4 (3) |
| O(49) | W(1) | C(4) | 97.8 (3) | W(1) | C(4) | C(3) | 133.8 (8) |
| O(49) | W(1) | C(5) | 95.4 (3) | W(1) | C(4) | C(5) | 74.2 (6) |
| N(7) | W(1) | C(4) | 159.6 (4) | W(2) | C(4) | C(3) | 142.4 (8) |
| N(7) | W(1) | C(5) | 162.9 (4) | W(2) | C(4) | C(5) | 68.7 (6) |
| C(4) | W(1) | C(5) | 36.4 (4) | C(3) | C(4) | C(5) | 133.6 (10) |
| W(1) | W(2) | O(37) | 113.8 (2) | W(1) | C(5) | W(2) | 75.0 (3) |
| W(1) | W(2) | O(43) | 114.9 (2) | W(1) | C(5) | C(4) | 69.4 (6) |
| W(1) | W(2) | O(49) | 52.8 (2) | W(1) | C(5) | C(6) | 131.1 (8) |
| W(1) | W(2) | N(31) | 138.1 (3) | W(2) | C(5) | C(4) | 72.5 (6) |
| W(1) | W(2) | C(4) | 53.7 (3) | W(2) | C(5) | C(6) | 146.3 (9) |
| W(1) | W(2) | C(5) | 55.8 (3) | C(4) | C(5) | C(6) | 131.7 (10) |
| O(37) | W(2) | O(43) | 119.8 (3) | | | | |

resonance superimposed on a broad hump in the *tert*-butyl region. However, on cooling to −80 °C, the spectrum shown in Figure 4 is obtained which is in accord with that expected from considerations of the solid-state molecular structure (Figure 3), although some other signals, subsequently identified as arising from $(t\text{-}BuO)_3W{\equiv}CH$, are present. There are eight resonances assignable to pyridine protons, three arising from the free half molecule of crystallization and the other five from coordinated pyridine. Evidently coordination of pyridine occurs with restricted rotation about the W–N bond leading to proximal and distal ortho and meta hydrogens as seen in the solid-state molecular structure. A molecular model reveals the steric congestion associated with this molecule and indicates the preferred alignment of the py blade, coincident with the M–M axis. At +10 °C, only three broad resonances are present in the pyridine region of the spectrum, indicating facile exchange between free and coordinated pyridine molecules.

Addition of pyridine-$d_5$ (ca. 100 equiv/$W_2$ complex) changes the temperature dependent appearance of the O-*t*-Bu resonances. At −1 °C, for example, there are four well-resolved O-*t*-Bu signals in the ratio 1:1:2:2 only slightly broadened from their low-temperature limiting appearance. We attribute these changes in the spectrum to a shift in the equilibrium $W_2(O\text{-}t\text{-}Bu)_6(py)(\mu\text{-}C_2H_2) \rightleftharpoons W_2(O\text{-}t\text{-}Bu)_6(\mu\text{-}C_2H_2) + py$, upon the addition of pyridine. This also suggests that O-*t*-Bu site exchange involves the unligated molecule $W_2(O\text{-}t\text{-}Bu)_6(\mu\text{-}C_2H_2)$ that could either have an unbridged (OR) structure or have two $\mu$-OR bridges as seen for $M_2(O\text{-}t\text{-}Bu)_6(\mu\text{-}CO)$ compounds, where M = Mo[17] or W,[18] in the solid state. The latter compounds show rapid O-*t*-Bu bridge ⇌ terminal site exchange even at −80 °C.

The $^1H$ chemical shifts of the $\mu\text{-}C_2R_2$ ligands are shifted downfield from the positions of the free alkyne $^1H$ resonances. For $\mu\text{-}C_2\mathit{Me}_2$, $\delta$ is 4.0 relative to $\delta$ 1.7 for free MeC≡CMe. For the $\mu\text{-}C_2H_2$ ligands, singlets are observed at $\delta$ 8.6 and 5.9 for the O-*i*-Pr and *t*-BuO compounds, respectively. Interestingly, no coupling $^2J_{^{183}W\text{-}C\text{-}^1H}$ is observed. However, as discussed below, $^1J_{^{183}W\text{-}^{13}C}$ is observed and it could be that the $^2J_{^{183}W\text{-}^1H}$ is too small to be detected.

**$^{13}C$ NMR Studies.** $^{13}C$ NMR spectra of labeled (90 atom % $^{13}C$) $W_2(O\text{-}t\text{-}Bu)_6(py)(\mu\text{-}{}^*C_2H_2)$ and $W_2(O\text{-}i\text{-}Pr)_6(py)_2(\mu\text{-}{}^*C_2H_2)$ have been recorded. The spectrum of the $\mu\text{-}{}^*C_2H_2$ ligand in the O-*t*-Bu complex is shown in Figure 5, and that of the O-*i*-Pr complex has a similar appearance. In the $^1H$-decoupled spectrum, the coordinated ethyne carbons appear as a singlet with coupling to $^{183}W$, $J_{W(1)\text{-}C} \simeq J_{W(2)\text{-}C} \simeq 44$ Hz. The $^1H$-coupled spectrum (Figure 6) is simpler than might have been anticipated for half of the expected AA′XX′ spectrum, and, for this reason, we have not as yet successfully extracted the coupling constants. However, we assume the coupling constants will be similar to, but smaller than, those found for $W_2(O\text{-}t\text{-}Bu)_6(CO)(\mu\text{-}{}^*C_2H_2)$ where we observe, in the ethyne region of the $^1H$ and $^{13}C$ spectra, the expected resonances for half of the AA′XX′ spectrum. The

(17) Chisholm, M. H.; Cotton, F. A.; Extine, M. W.; Kelly, R. L. *J. Am. Chem. Soc.* **1979**, *101*, 7645.
(18) Chisholm, M. H.; Hoffman, D. M., unpublished results.

Table VI. Selected Bond Distances (Å) and Angles (deg) for the $W_2(O\text{-}t\text{-}Bu)_6(py)(\mu\text{-}C_2H_2)$ Molecule

| A | B | dist | A | B | dist |
|---|---|---|---|---|---|
| W(1) | W(2) | 2.665 (1) | W(2) | O(5) | 1.999 (6) |
| W(1) | O(5) | 2.083 (6) | W(2) | O(31) | 1.924 (6) |
| W(1) | O(10) | 1.958 (6) | W(2) | O(36) | 1.914 (6) |
| W(1) | O(15) | 1.928 (6) | W(2) | N(25) | 2.267 (8) |
| W(1) | O(20) | 1.927 (6) | W(2) | C(3) | 2.090 (10) |
| W(1) | C(3) | 2.119 (9) | W(2) | C(4) | 2.093 (9) |
| W(1) | C(4) | 2.095 (9) | C(3) | C(4) | 1.441 (14) |

| A | B | C | angle | A | B | C | angle |
|---|---|---|---|---|---|---|---|
| W(2) | W(1) | O(5) | 47.9 (2) | O(5) | W(2) | O(36) | 95.2 (3) |
| W(2) | W(1) | O(10) | 142.0 (2) | O(5) | W(2) | N(25) | 177.5 (3) |
| W(2) | W(1) | O(15) | 108.5 (2) | O(5) | W(2) | C(3) | 97.8 (3) |
| W(2) | W(1) | O(20) | 107.7 (2) | O(5) | W(2) | C(4) | 97.9 (3) |
| W(2) | W(1) | C(3) | 50.2 (3) | O(31) | W(2) | O(36) | 115.1 (3) |
| W(2) | W(1) | C(4) | 50.4 (3) | O(31) | W(2) | N(25) | 84.4 (3) |
| O(5) | W(1) | O(10) | 170.1 (2) | O(31) | W(2) | C(3) | 100.6 (3) |
| O(5) | W(1) | O(15) | 86.6 (2) | O(31) | W(2) | C(4) | 140.1 (3) |
| O(5) | W(1) | O(20) | 86.2 (3) | O(36) | W(2) | N(25) | 82.6 (3) |
| O(5) | W(1) | C(3) | 94.4 (3) | O(36) | W(2) | C(3) | 140.5 (3) |
| O(5) | W(1) | C(4) | 95.2 (3) | O(36) | W(2) | C(4) | 101.0 (3) |
| O(10) | W(1) | O(15) | 88.4 (3) | N(25) | W(2) | C(3) | 84.7 (3) |
| O(10) | W(1) | O(20) | 89.3 (3) | N(25) | W(2) | C(4) | 83.8 (3) |
| O(10) | W(1) | C(3) | 94.8 (3) | C(3) | W(2) | C(4) | 40.3 (4) |
| O(10) | W(1) | C(4) | 94.2 (3) | W(1) | O(5) | W(2) | 81.5 (2) |
| O(15) | W(1) | O(20) | 122.7 (3) | W(1) | O(5) | C(6) | 139.6 (5) |
| O(15) | W(1) | C(3) | 98.1 (3) | W(2) | O(5) | C(6) | 138.9 (5) |
| O(15) | W(1) | C(4) | 138.1 (3) | W(1) | O(10) | C(11) | 144.8 (6) |
| O(20) | W(1) | C(3) | 139.2 (3) | W(1) | O(15) | C(16) | 151.1 (6) |
| O(20) | W(1) | C(4) | 99.2 (3) | W(1) | O(20) | C(21) | 151.2 (6) |
| C(3) | W(1) | C(4) | 40.0 (4) | W(2) | O(31) | C(32) | 151.9 (6) |
| W(1) | W(2) | O(5) | 50.6 (2) | W(2) | O(36) | C(37) | 152.9 (6) |
| W(1) | W(2) | O(31) | 118.6 (2) | W(1) | C(3) | W(2) | 78.6 (3) |
| W(1) | W(2) | O(36) | 117.1 (2) | W(1) | C(3) | C(4) | 69.1 (5) |
| W(1) | W(2) | N(25) | 131.6 (2) | W(2) | C(3) | C(4) | 69.9 (6) |
| W(1) | W(2) | C(3) | 51.2 (3) | W(1) | C(4) | W(2) | 79.0 (3) |
| W(1) | W(2) | C(4) | 50.5 (2) | W(1) | C(4) | C(3) | 70.9 (5) |
| O(5) | W(2) | O(31) | 95.4 (3) | W(2) | C(4) | C(3) | 69.7 (5) |

Table VII. Angles Subtended by Trigonal Bipyramidally Coordinated Tungsten Atoms Assuming the $\mu\text{-}C_2R_2$ Ligand To Occupy One Position, CTR, at the Midpoint of the C–C Bond

| compd | atom | atom | atom | angle, deg | assignt |
|---|---|---|---|---|---|
| $W_2(O\text{-}t\text{-}Bu)_6(\mu\text{-}C_2H_2)(py)$ | O(20) | W(1) | O(15) | 123 | ee |
| | O(20) | W(1) | CTR | 119 | ee |
| | O(15) | W(1) | CTR | 118 | ee |
| | O(20) | W(1) | O(10) | 89 | ee |
| | O(20) | W(1) | O(5) | 86 | ae |
| | O(15) | W(1) | O(10) | 88 | ae |
| | O(15) | W(1) | O(15) | 87 | ae |
| | O(10) | W(1) | CTR | 95 | ae |
| | O(5) | W(1) | CTR | 95 | ae |
| | O(10) | W(1) | O(5) | 170 | aa |
| | O(36) | W(2) | O(31) | 115 | ee |
| | O(36) | W(2) | CTR | 121 | ee |
| | O(31) | W(2) | CTR | 120 | ee |
| | O(36) | W(2) | O(5) | 95 | ae |
| | O(36) | W(2) | N(25) | 83 | ae |
| | O(31) | W(2) | O(5) | 95 | ae |
| | O(31) | W(2) | N(25) | 84 | ae |
| | CTR | W(2) | O(5) | 98 | ae |
| | CTR | W(2) | N(25) | 84 | ae |
| | O(5) | W(2) | N(25) | 177 | aa |
| $W_2(OCH_2\text{-}t\text{-}Bu)_6(py)_2\text{-}(\mu\text{-}C_2Me_2)$ | O(37) | W(2) | CTR | 119 | ee |
| | O(37) | W(2) | O(43) | 120 | ee |
| | CTR | W(2) | O(43) | 118 | ee |
| | O(37) | W(2) | O(49) | 91 | ae |
| | O(37) | W(2) | N(31) | 84 | ae |
| | CTR | W(2) | O(49) | 105 | ae |
| | CTR | W(2) | N(31) | 86 | ae |
| | O(43) | W(2) | O(49) | 91 | ae |
| | O(43) | W(2) | N(31) | 83 | ae |
| | O(49) | W(2) | N(31) | 169 | aa |

coupling constants are $^1J_{CH}$ = 192 Hz, $^2J_{CH}$ = −1.7 Hz, $^1J_{CC}$ = 15.8 Hz, and $^3J_{HH}$ = 5.4 Hz. The relative signs of $^1J_{CH}$ and $^2J_{CH}$ are necessarily opposite (we chose $^2J_{CH}$ negative), and the relative signs of $^1J_{CC}$ and $^3J_{HH}$ remain undetermined. The $^2J_{CH}$ value is small in the CO adduct so the peak separation (184 Hz) in Figure 6 for the pyridine complex should be close to $^1J_{CH}$.

The coupling constants observed $W_2(O\text{-}t\text{-}Bu)_6(CO)(\mu\text{-}{}^*C_2H_2)$ are intriguing. The $^1J_{CH}$ value of 192 Hz is between that for organic ethylene ($^1J_{CH}$ = 156 Hz) and ethyne ($^1J_{CH}$ = 249 Hz) and is comparable to that found for the strained ring systems cyclopropane ($^1J_{CH}$ = 161 Hz) and bicyclobutane ($^1J_{CH}$ = 205 Hz).[19] The observed two-bond C–H coupling constant is similar to that found in ethylene ($^2J_{CH}$ = −2.4 Hz) and cyclopropane ($^2J_{CH}$ = −2.6 Hz). Most interestingly, the $^{13}C$–$^{13}C$ coupling constant of 15.8 Hz is very small ($J_{CC}$ = 35, 68, and 172 Hz for ethane, ethylene, and ethyne, respectively) and is best compared to the value observed in three member organic ring systems (ca. 10 Hz).[19] The observed coupling constants for the coordinated ethyne, especially the small $^{13}C$–$^{13}C$ value, support the dimetallatetrahedrane paradigm for these ditungsten species.

**Identification of the W≡CH Group.** During the course of $^{13}C$ NMR studies of $W_2(O\text{-}t\text{-}Bu)_6(py)(\mu\text{-}{}^*C_2H_2)$, a signal at δ 252.4 with coupling to $^{183}W$, $J_{W-^{13}C}$ = 289 Hz and $J_{^{13}C-^1H}$ = 150 Hz, was discovered. (See Figure 5.) The chemical shift and coupling constants reliably establish this as arising from a W≡*CH group. A comparison of NMR data with related tungsten alkylidyne complexes is shown in Table VIII. The tungsten satellites have the proper intensity for coupling to one tungsten-183 nucleus, 14.3% natural abundance.

The observed $^{13}C$–$^1H$ coupling constant led us to identify the methylidyne proton resonance in the $^1H$ NMR spectrum of $^{13}C$ labeled and unlabeled $W_2(O\text{-}t\text{-}Bu)_6(py)(\mu\text{-}C_2H_2)$: δ(CH) = 5.47 with $^2J_{^{183}W-^1H}$ = 90 Hz. Again, these parameters are comparable

(19) Marshall, J. L. *Methods Stereochem. Anal.* **1983**, *2*, 11. Stothers, J. B. "Carbon-13 NMR Spectroscopy"; Academic Press: New York, **1972**. Gunther, H. *Angew. Chem., Int. Ed. Engl.* **1972**, *11*, 861.

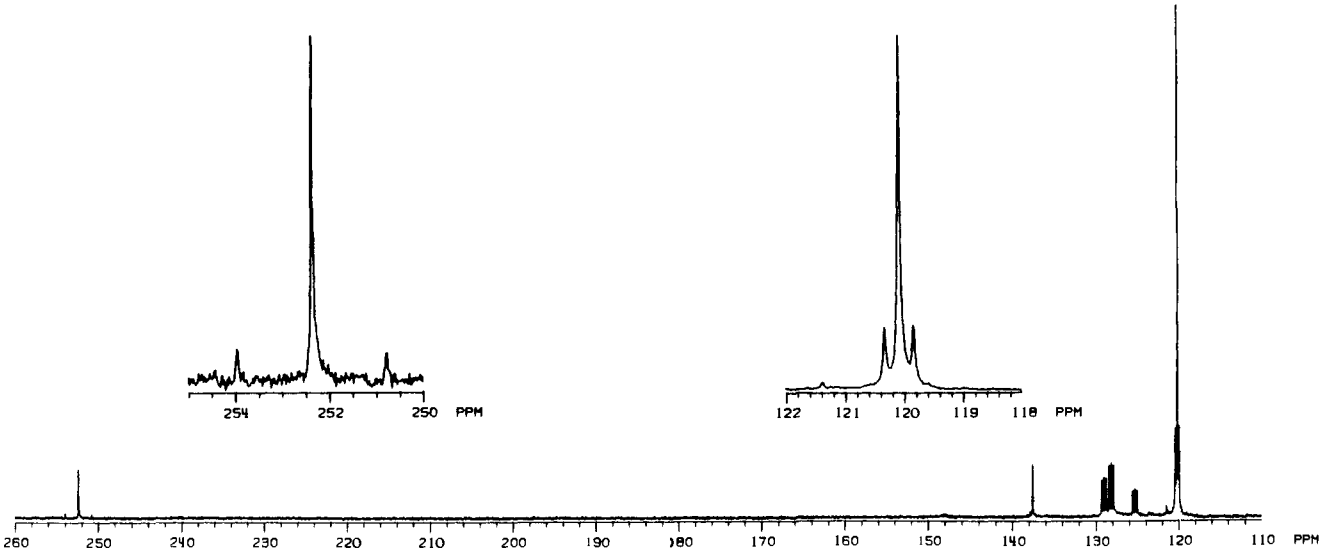


**Figure 5.** Proton-decoupled $^{13}C$ NMR spectrum of a crystalline sample of $W_2(O\text{-}t\text{-}Bu)_6(py)(\mu\text{-}{}^*C_2H_2)\cdot{}^1/_2py$, where *C represents 90 atom % $^{13}C$, dissolved in toluene-$d_8$ recorded at −40 °C, 90 MHz, in the region 260–110 ppm. The resonances arising from the $W_2(\mu\text{-}{}^*C_2H_2)$ ($\delta$ 120.1) and W≡*CH ($\delta$ 252.4) groups are shown at scale expansion in the insets. The signals in the region $\delta$ 124–138 arise from the ring carbons of the solvent.

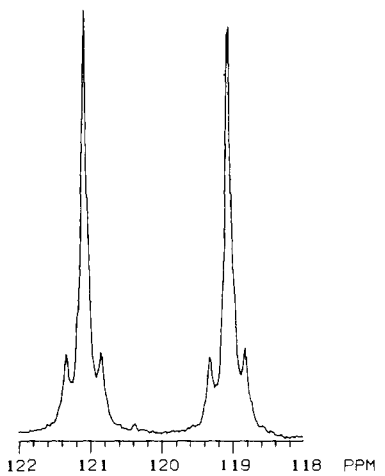


**Figure 6.** Proton-coupled $^{13}C$ NMR spectrum in the $W_2(\mu\text{-}{}^*C_2H_2)$ region for the $W_2(O\text{-}t\text{-}Bu)_6(py)(\mu\text{-}{}^*C_2H_2)\cdot{}^1/_2py$ sample in toluene-$d_8$, at 90 MHz and at −40 °C.

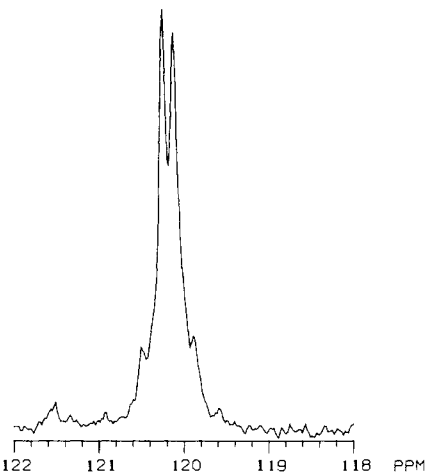


**Figure 7.** Proton-decoupled $^{13}C$ NMR spectrum in the $W_2(\mu\text{-}C_2H_2)$ region of the sample formed by dissolving roughly equal molar quantities of $W_2(O\text{-}t\text{-}Bu)_6(py)(\mu\text{-}{}^*C_2H_2)\cdot{}^1/_2py$ and $W_2(O\text{-}t\text{-}Bu)_6(py)(\mu\text{-}C_2D_2)\cdot{}^1/_2py$ in toluene-$d_8$, recorded at 90 MHz and at −40 °C.

with those obtained for other tungsten methylidyne complexes. In addition to the W≡CH resonances, a singlet close to one of the O-*t*-Bu proton signals is always present in the $^1H$ spectra of $W_2(O\text{-}t\text{-}Bu)_6(py)(\mu\text{-}C_2H_2)$. On the basis of the relative intensities of the signals associated with the $W_2(\mu\text{-}C_2H_2)$ and W≡CH moieties (10:1), both in the $^1H$ and $^{13}C$ spectra, we can estimate their relative concentrations to be $W_2(\mu\text{-}C_2H_2)$: W≡CH ca. 5:1. Since the spectra recorded for both labeled and unlabeled compounds were obtained from crystalline samples, the repeated appearance of the W≡CH signal in ca. 10% relative intensity is interesting. Two plausible explanations were considered. (1) The $W_2(\mu\text{-}C_2H_2)$ compound decomposes to give the W≡CH compound. (2) The $W_2(\mu\text{-}C_2H_2)$ and the W≡CH containing compounds are in equilibrium. On the basis of the metathetic reactions (1), the dimer structure of $[(t\text{-}BuO)_3W{\equiv}CMe]_2$,[20] and the lability of py to reversibly coordinate to tungsten alkoxide complexes, the essential features of the equilibrium could take the form of eq 3.

$$W_2(O\text{-}t\text{-}Bu)_6(\mu\text{-}C_2H_2) \rightleftharpoons [(t\text{-}BuO)_3W{\equiv}CH]_2 \qquad (3)$$

**Evidence for the Equilibrium between the Dimetallatetrahedrane and the Methylidynemetal Complex.** Many of the classical approaches to demonstrating the existence of a chemical equilibrium are thwarted in the present instance by the thermal instability of $W_2(O\text{-}t\text{-}Bu)_6(py)(\mu\text{-}C_2H_2)$ in hydrocarbon solutions (discussed later). However, within the temperature range 0 to −60 °C, the relative concentrations of W≡*CH and $W_2(\mu\text{-}{}^*C_2H_2)$ appeared relatively constant. It could be that $K_{eq}$ for (3) is relatively insensitive to temperature change or that at these temperatures the concentrations of the two species are essentially frozen at an equilibrium position determined by the initial preparation of the NMR sample at room temperature. At +35 °C, the decomposition of $W_2(O\text{-}t\text{-}Bu)_6(py)(\mu\text{-}C_2H_2)$ is essentially complete within 1.5 h. Spectra recorded on $^{13}C$-labeled samples during this period revealed significantly higher concentrations of the W≡*CH signal, relative to the $W_2(\mu\text{-}{}^*C_2H_2)$ signal, but it is not clear how this observation should be interpreted. Consequently we attempted to test the hypothesis that there exists an equilibrium of the type described by eq 3, involving the reversible metathesis of W–W and C–C bonds, by chemical reactions.

Roughly equal molar quantities of crystalline $W_2(O\text{-}t\text{-}Bu)_6(py)(\mu\text{-}{}^{13}C_2H_2)$ and $W_2(O\text{-}t\text{-}Bu)_6(py)(\mu\text{-}C_2D_2)$ were combined and dissolved in toluene-$d_8$ in an NMR tube. The tube was sealed and the solution was allowed to stand at room temperature for 15–20 min before being placed in the probe (at −40 °C) of the Nicolet 360 NMR spectrometer. The $^{13}C$ NMR spectrum was recorded at −40 °C and showed, in addition to the signal for the W≡*CH moiety, two resonances in the $W_2(\mu$-ethyne) region, as

(20) Chisholm, M. H.; Hoffman, D. M.; Huffman, J. C. *Inorg. Chem.* **1983**, *22*, 2903.

shown in Figure 7, at $\delta$ 120.2 and 120.1 ($\Delta\nu$ = 11.2 Hz) in the relative intensity ratio of approximately 1:1. Each resonance is flanked by tungsten satellites. We ascribe the appearance of the low-field resonance to the $W_2(\mu$-H*CCD) species. The separation of the two signals arising from $W_2(\mu$-H*C*CH) and $W_2(\mu$-H*CCD), 11.2 Hz, is within the range expected for a secondary isotope effect. We can discount the mere scrambling of H and D that would lead to W≡*CH/D and $\mu$-*$C_2HD$, $\mu$-*$C_2D_2$ by the lack of $^{13}C$–$^2H$ coupling in the $^{13}C$ NMR spectra and also because, in the $^1H$ NMR spectrum of the above sample, we would have seen formation of $\mu$-$C_2H_2$ and $\mu$-$C_2HD$ ligands[21] in addition to the resonances due to $\mu$-*$C_2H_2$. The above experiment reliably identifies the kinetically facile equilibrium (4).

$$W_2(O\text{-}t\text{-}Bu)_6(py)(\mu\text{-H*C*CH}) + W_2(O\text{-}t\text{-}Bu)_6(py)(\mu\text{-DCCD}) \rightleftharpoons 2W_2(O\text{-}t\text{-}Bu)_6(py)(\mu\text{-H*CCD}) \quad (4)$$

The relative intensities of the $\mu$-ethyne signals at ca. 120 ppm are roughly in the ratio 1:1 as expected, since for $W_2(\mu$-H*C*CH) there are two $^{13}C$ atoms and for $W_2(\mu$-H*CCD) there is only one, but the latter is favored by a factor of 2 according to eq 4. Thus, within 15–20 min, equilibrium 4 must be reached at room temperature. If (3) is a kinetically facile equilibrium at room temperature, then the rapid scrambling of (4) must follow, but the observation of (4) does not constitute proof of equilibrium 3. It is possible that (4) occurs by some other pathway. One alternate pathway involves the ethyne metathesis sequence shown in eq 5.

$$W_2(O\text{-}t\text{-}Bu)_6(\mu\text{-*}C_2H_2) \rightleftharpoons W_2(O\text{-}t\text{-}Bu)_6 + *C_2H_2 \quad (5i)$$

$$(t\text{-BuO})_3W{\equiv}CD + H*C*CH \rightleftharpoons (t\text{-BuO})_3W{\equiv}*CH + H*CCD \quad (5ii)$$

In (5), the methylidyne complex is an alkyne metathesis catalyst[22] and the rapid attainment of equilibrium 4 relies upon a kinetically labile and reversible alkyne dissociation step, (5i). We rule out (5i) on the following grounds. (1) When a solution of freshly prepared $W_2(O\text{-}t\text{-}Bu)_6(py)(\mu\text{-}C_2H_2)$ in toluene-$d_8$ was subject to three successive cycles of "freeze, thaw, and pump" during which the sample was warmed to room temperature for 5 min between each cycle, no evidence for the formation of $W_2(O\text{-}t\text{-}Bu)_6$ was observed. (2) If ethyne dissociation were to occur (5i), we would expect to see formation of $W_2(O\text{-}t\text{-}Bu)_6$, $W_2(O\text{-}t\text{-}Bu)_6(\mu\text{-}C_4H_4)$, and polyacetylene during the decomposition of $W_2(O\text{-}t\text{-}Bu)_6(py)(\mu\text{-}C_2H_2)$.[23] (3) Addition of 1 equiv of $C_2D_2$ to a toluene-$d_8$ solution of $W_2(O\text{-}t\text{-}Bu)_6(py)(\mu\text{-*}C_2H_2)$ in an NMR tube at −198 °C, followed by warmup to room temperature, 10 min, and subsequent cooling to −40 °C revealed, by $^{13}C$ NMR spectroscopy, the formation of $W_2(O\text{-}t\text{-}Bu)_6(\mu\text{-}C_4H_2D_2)$ with the connectivity in the $\mu$-$C_4H_2D_2$ ring being reliably established as that in III by $^{13}C$–$^{13}C$ and $^{13}C$–$^1H$ couplings. Only a trace of $W_2(O\text{-}t\text{-}Bu)_6(py)(\mu\text{-*}C_2H_2)$ remained, and this was not isotopically scrambled. (4) Finally, when a solution of $W_2(O\text{-}t\text{-}Bu)_6(py)(\mu\text{-*}C_2H_2)$ in hexane at room temperature was exposed to CO, 1 equiv, and then stripped to dryness in vacuo and the solids

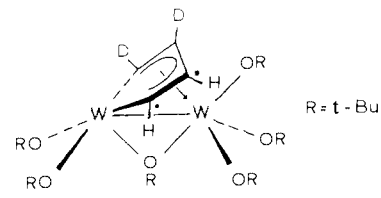


III

redissolved in toluene-$d_8$ and examined by $^1H$ and $^{13}C$ NMR spectroscopy, *only* resonances assignable to the compound $W_2(O\text{-}t\text{-}Bu)_6(CO)(\mu\text{-*}C_2H_2)$ were detected. The structure of the latter compound is not known, but spectroscopic data are consistent with that shown schematically in IV, i.e., an analogue of the py adduct shown in Figure 3. A notable difference in solution is that the CO ligand remains bound on the NMR time scale resulting in a nonfluxional molecule.

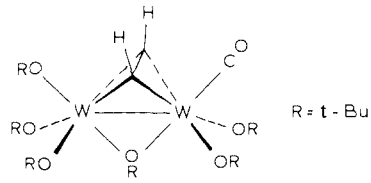


IV

All of the above are consistent with the existence of a facile equilibrium, (3) but do not constitute proof of the same, though we can think of no likely alternative explanation(s). Interestingly, no evidence for methylidyne formation is observed for the isopropoxy ethyne compound $W_2(O\text{-}i\text{-}Pr)_6(py)_2(\mu\text{-}C_2H_2)$.[21]

**Thermal Decomposition of $W_2(\mu\text{-}C_2H_2)(OR)_6$ Compounds.** The ultimate products of decomposition of $W_2(O\text{-}t\text{-}Bu)_6(py)(\mu\text{-*}C_2H_2)$ do not include the methylidyne complex discussed previously. The green solution of $W_2(O\text{-}t\text{-}Bu)_6(py)(\mu\text{-*}C_2H_2)$ changes to a dark red, and the $^{13}C$ NMR spectrum (−40 °C) of the decomposition products (1 day, 25 °C) reveal a number of signals with chemical shifts greater than (downfield of) $\delta$ 150. One signal, at $\delta$ 273, is of much greater intensity than the others (ca. 75% of total intensity below $\delta$ 150). The signal shows coupling to $^{183}W$, $J_{W-^{13}C}$ = 147 Hz, and to $^1H$, $J_{^{13}C-H}$ = 163 Hz. The intensities of the tungsten satellites indicate a coupling to two $^{183}W$ nuclei that, together with the magnitude of $J_{W-C}$, is consistent with the existence of a $W_2(\mu$-*CH) moiety. In the $^1H$ NMR spectrum of the decomposed $^{13}C$-labeled compound, there is a plethora of *t*-BuO signals, as well as resonances assignable to isobutylene and a resonance at $\delta$ 16.9 with $J_{^{13}C-^1H}$ = 163 Hz (assignable to $W_2(\mu$-C*H*)).

The appearance of isobutylene indicates that W=O groups are being formed: $M(O\text{-}t\text{-}Bu)_2 \rightarrow MO + (Me_2)C{=}CH_2 + t\text{-BuOH}$. The above finding is thus relevant to the observation of Cotton and co-workers,[25] who have isolated an oxo, $\mu$-alkylidyne complex, $[W_3(O\text{-}t\text{-}Bu)_5(\mu\text{-O})(\mu\text{-CEt})O]_2$, from the heated reaction between $W_2(O\text{-}t\text{-}Bu)_6$ and EtC≡CEt.

The thermal decomposition products of $W_2(O\text{-}i\text{-}Pr)_6(py)_2(\mu$-*$C_2H_2$) are no less intriguing. Although the isopropoxy complex does not decompose rapidly at room temperature, when heated to +90 °C for 1 h (toluene-$d_8$, sealed NMR tube), the decomposition is complete. A discussion of the decomposition products derived from $W_2(O\text{-}i\text{-}Pr)_6(py)_2(\mu\text{-}C_2H_2)$ will have to await isolation and characterization of one or more of the compounds. However, we can say that we do not observe formation of soluble methylidyne compounds to any significant extent, but we do see formation of what we believe to be tungsten carbide or acetylide compounds based on the appearance of low-field $^{13}C$ signals lacking coupling to $^1H$ nuclei.

**Concluding Remarks.** (1) Ditungsten hexaalkoxides react with alkynes to give products that are determined by steric factors

(21) In an analogous experiment, $W_2(O\text{-}t\text{-}Bu)_6(py)(\mu\text{-}C_2H_2)$ and $W_2(O\text{-}t\text{-}Bu)_6(py)(\mu\text{-}C_2D_2)$ were mixed and dissolved in toluene-$d_8$ and the $^1H$ NMR spectrum was recorded. This spectrum showed, in addition to the $^1H$ signal assignable to W≡CH, two singlets in the $\mu$-ethyne region in roughly equal intensity ratio ($\Delta\nu$ = 7.2 Hz) assignable to $\mu$-HCCH and $\mu$-HCCD ligands. In this experiment, one cannot distinguish between C–H/D and C–C scrambling, but it does provide further support for the arguments and assignments presented in the double label experiment. Also, when equimolar quantities of $W_2(O\text{-}i\text{-}Pr)_6(py)_2(\mu\text{-}C_2H_2)$ and $W_2(O\text{-}i\text{-}Pr)_6(py)_2(\mu\text{-}C_2D_2)$ were mixed and dissolved in toluene-$d_8$, the $^1H$ NMR spectrum showed only a single resonance in the bridging ethyne region: no $\mu$-$C_2HD$ was detectable.

(22) Sancho, J.; Schrock, R. R. *J. Mol. Catal.* **1982**, *15*, 75. Schrock, R. R. *ACS Symp. Ser.* **1983**, *211*, 369 and references therein.

(23) The compound $Mo_2(O\text{-}i\text{-}Pr)_6(py)_2(\mu\text{-}C_2Me_2)$ was previously shown to decompose by this route giving hexamethylbenzene, $Mo_2(O\text{-}i\text{-}Pr)_6$, and py. See: ref 3.

(24) This is a characteristic mode of decomposition: Bradley, D. C.; Mehrotra, R. C.; Gaur, P. D. "Metal Alkoxides"; Academic Press: New York, 1978.

(25) Cotton, F. A.; Schwotzer, W.; Shamshoum, E. S. *Organometallics* **1983**, *2*, 1340.

**Table VIII.** Relevant $^{13}C$ NMR Data for W–C Bonds in Selected Tungsten Complexes

| compd | $^{13}C$ chem shift | $J_{WC}$, Hz | $^{1}J_{CH}$, Hz | ref |
|---|---|---|---|---|
| $W_2(O\text{-}i\text{-}Pr)_6(py)_2(HCCH)$ | 166.3 | 41.6 | 192[a] | this work |
| $W_2(O\text{-}t\text{-}Bu)_6(py)(HCCH)\cdot{}^1/_2py$ | 120.1 | 44.1[b] | 184[a] | this work |
| $W_2(O\text{-}t\text{-}Bu)_6(CO)(HCCH)$ | 125.5 | 38, 25.1 | 191.9 | this work |
| $W(CCMe_3)(CHCMe_3)(CH_2CMe_3)(PMe_3)_2$ | 316 (≡C) | 210 | | *c* |
| | 286 (=C) | 120 | 90 | |
| | 53.5 (—C) | 80 | 113 | |
| $W(CCMe_3)(CH_2CMe_3)_3$ | 317 (≡C) | 230 | | *d* |
| | 103.7 (—C) | 89 | 115 | |
| $W(CH)(Cl)(PMe_3)_4$ | 250 (≡C) | 200 | 134 | *e* |
| *trans*-$W(CCMe_3)(dmpe)_2(H)$ | 281.6 | 208 | | *f* |
| *trans*-$W(CCMe_2)(dmpe)_2Cl$ | 271.1 (≡C) | NG | | *f* |
| $[W(CCMe_3)(dmpe)_2(H)Cl]Cl$ | 285.5 (≡C) | NG | | *f* |
| $W(CCMe_3)(PMe_3)_4Cl$ | 271 (≡C) | NG | | *f* |
| $W(CH)(dmpe)_2Cl$ | 246.2 (≡C) | 205 | 130 | *f* |
| $[W(CH)(H)(dmpe)_2Cl]Cl$ | 263.6 (≡C) | | 125 | *f*, *g* |
| $W(CCMe_3)(CHCMe_3)(CH_2CMe_3)(dmpe)$ | 296 (≡C) | NG | | *c* |
| | 256 (=C) | NG | 84 | |
| | 54.7 (—C) | NG | NG | |
| $W(CMe)Me(PMe_3)_4$ | 251 | NG | | *h* |
| $W(CPh)(PMe_3)_3Cl_3$ | 357 (≡C) | NG | | *i* |
| $W(CPh)(OCMe_3)_3$ | 257 (≡C) | NG | | *i* |
| $W(CCMe_3)X_3$ | | | | |
| X = $OCMe_3$ | 271 (≡C) | NG | | *i* |
| X = $NMe_2$ | 288 (≡C) | NG | | *j* |
| X = $SCMe_3$ | 335 (≡C) | NG | | *j* |
| $W(CCMe_3)(OMe)_3(NMe_2H)_2$ | 286 (≡C) | NG | | *j* |
| $[PEt_3H][W(CCMe_3)Cl_4]$ | 339 (≡C) | 205 | | *j* |
| $[NEt_4][W(CCMe_3)Cl_4]$ | 337 (≡C) | NG | | *j* |
| $[NEt_4][W(CCMe_3)(PEt_3)Cl_4]$ | 335 (≡C) | NG | | *j* |
| $W(CCMe_3)(dme)Cl_3$ | 335 (≡C) | 224 | | *j* |
| $W(CCMe_3)(Et_3PO)Cl_3$ | 329 (≡C) | 208 | | *j* |
| $W(CCMe_3)(Et_3PO)(PEt_3)Cl_3$ | 340 (≡C) | NG | | *j* |
| $W(CCMe_3)(PMe_3)_3Cl_3$ | 401 (≡C) | NG | | *j* |
| $W(CCMe_3)(PMe_3)_2Cl_3$ | 357 (≡C) | NG | | *j* |
| $W(CCMe_3)(PMe_3)Cl_3$ | 345 (≡C) | NG | | *j* |
| $W(CCMe_3)(PEt_3)Cl_3$ | 346 (≡C) | 209 | | *j* |
| $W(CSiMe_3)(CH_2SiMe_3)_3$ | 344.6 (≡C) | NG | | *d* |
| | 56.2 (—C) | 81 | NG | |
| $W_2(\mu\text{-}CSiMe_3)_2(CH_2SiMe_3)_4$ | 352.6 (≡C) | 73 | | *k* |
| | 68.9 (—C) | 74 | | |
| $W(CMe)(CO)_4X$ | | | | |
| X = Br | 288 (≡C) | 178.2 | | *l* |
| X = Cl | 289 (≡C) | 168.5 | | |
| $W(O)(CHR)(PEt_3)_2Cl_2$ | | | | |
| R = $CMe_3$ | 313.3 (=C) | 148 | 126 | *m* |
| R = Ph | 291.6 (=C) | NG | 117 | *m* |
| R = H | 281.1 (=C) | NG | ~136 | *m* |
| $W(O)(CHCMe_3)(PEt_3)Cl_2$ | 295.4 (=C) | 176 | 115 | *n* |
| $W_2Me_2(NEt_2)_4$ | 25–30 (—C) | ~114.0 | NG | *o* |
| $W_2(CH_2SiMe_3)_6$ | 77.1 (—C) | 78.0 | NG | *k* |

[a] Approximate value; NG = not given. [b] $J_{W_1C} \simeq J_{W_2C}$. [c] Clark, D. N.; Schrock, R. R. *J. Am. Chem. Soc.* **1978**, *100*, 6774. [d] Andersen, R. A.; Chisholm, M. H.; Gibson, J. F.; Reichert, W. W.; Rothwell, I. P.; Wilkinson, G. *Inorg. Chem.* **1981**, *20*, 3934. [e] Sharp, P. R.; Holmes, S. J.; Schrock, R. R.; Churchill, M. R.; Wasserman, H. J. *J. Am. Chem. Soc.* **1981**, *103*, 965. [f] Holmes, S. J.; Clark, D. N.; Turner, H. W.; Schrock, R. R. *J. Am. Chem. Soc.* **1982**, *104*, 6322. [g] Data obtained at 243 K, $CD_2Cl_2$. Represents frozen out methylidyne–hydride complex which, at higher temperatures, is in rapid exchange with a methylidene complex. [h] Chiu, K. W.; Jones, R. A.; Wilkinson, G.; Galar, A. M. R.; Hursthouse, M. B.; Malik, K. M. A. *J. Chem. Soc. Dalton Trans.* **1981**, 1204. [i] Wengrovius, J. H.; Sancho, J.; Schrock, R. R. *J. Am. Chem. Soc.* **1981**, *103*, 3932. [j] Schrock, R. R.; Clark, D. N.; Sancho, J.; Wengrovius, J. H.; Rocklage, S. M.; Pedersen, S. F. *Organometallics* **1982**, *1*, 1645. [k] Chisholm, M. H.; Cotton, F. A.; Extine, M. W.; Stults, B. R. *Inorg. Chem.* **1976**, *15*, 2252. [l] Kohler, F. H.; Kalder, H. J.; Fischer, E. O. *J. Organomet. Chem.* **1976**, *113*, 11. [m] Schrock, R. R.; Rocklage, S.; Wengrovius, J.; Rupprecht, G.; Fellmann, J. *J. Mol. Catal.* **1980**, *8*, 73. [n] Wengrovius, J. H.; Schrock, R. R.; Churchill, M. R.; Missert, J. R.; Youngs, W. J. *J. Am. Chem. Soc.* **1980**, *102*, 4515. [o] Chisholm, M. H.; Cotton, F. A.; Extine, M. W.; Millar, M.; Stults, B. R. *Inorg. Chem.* **1976**, *15*, 2244 (anti ⇌ gauche).

associated with the alkoxy group and the substituents on the alkyne.

(2) The alkyne adducts $W_2(O\text{-}t\text{-}Bu)_6(py)(\mu\text{-}C_2H_2)$, $W_2(O\text{-}i\text{-}Pr)_6(py)_2$ ($\mu\text{-}C_2H_2$), and $W_2(OCH_2\text{-}t\text{-}Bu)_6(py)_2(\mu\text{-}C_2Me_2)$ adopt structures and show solution behavior (VT NMR) that reflect the steric crowding of the molecules. On the basis of M–M and C–C distances, the compound $W_2(O\text{-}t\text{-}Bu)_6(py)(\mu\text{-}C_2H_2)$ contains the closest approach, thus far seen in organometallic chemistry, to a dimetallahedrane.

(3) A number of experimental observations are consistent with the existence of an equilibrium between a dimetallatetrahedrane and a methylidyne complex (eq 3). By appropriate variations of alkoxy groups and acetylenic substituents, it should be possible to probe this matter more exactly. Previously, the fragmentation of a $\mu$-alkyne ligand on a cluster to give two $\mu$-alkylidyne ligands[26] and the reverse, the coupling of two terminal M≡CR groups to give a $M_2(\mu\text{-}C_2R_2)$ moiety, have been noted.[27] However, a facile equilibrium of the type shown in eq 3 is unprecedented.

(26) Park, J. T.; Shapley, J. R.; Churchill, M. R.; Bueno, C. *J. Am. Chem. Soc.* **1983**, *105*, 6182 and references therein. Shapley, J. R.; Hoffmann, R.; et al. *Organometallics* **1984**, *3*, 619.

(27) Fischer, E. O.; Ruhs, A.; Friedrich, P.; Huttner, G. *Angew. Chem., Int. E. Engl.* **1977**, *16*, 465.

(28) Huffman, J. C.; Lewis, L.; Caulton, K. G. *Inorg. Chem.* **1980**, *19*, 2755. Chisholm, M. H.; Folting, K.; Huffman, J. C.; Kirkpatrick, C. C. *Inorg. Chem.*, in press.

Futher studies are in progress.[29]

## Experimental Section

**Reagents and General Techniques.** General procedures and the preparations of $W_2(OR_6(py)_2$, R = *i*-Pr and $CH_2$-*t*-Bu, and $W_2(O$-*t*-Bu$)_6$ have been described.[6] 2-Butyne was purchased from Farchan and degassed prior to use. Ethyne was purchased from Matheson and was used without purification. Dry and oxygen-free hexane, toluene, and pyridine were used in all preparations. Elemental analyses were performed by Alfred Bernhardt Microanalytisches Laboratorium, West Germany.

$^1$H NMR spectra were recorded on a Nicolet NT-360 360-MHz spectrometer in dry and oxygen-free toluene-$d_8$. $^{13}$C NMR spectra were recorded on the same instrument at 90-MHz in toluene-$d_8$. The $^{13}$C NMR spectra were obtained for the $\mu$-ethyne complexes using the labeled (ethyne-*1,2*-$^{13}C_2$ 90 atom % $^{13}$C) crystalline complexes prepared as described below. The $^{13}$C labeled ethyne was purchased from MSD Isotopes and used without purification. All $^1$H NMR chemical shifts are in parts per million relative to the $CHD_2$ quintet of toluene-$d_8$ set at $\delta$ 2.090. $^{13}$C NMR chemical shifts are in parts per million relative to the ipso carbon of toluene-$d_8$ set at $\delta$ 137.5. The $^{13}$C–$^1$H coupling constants reported were obtained by using gated $^1$H decoupling techniques.

Infrared spectra were obtained on a Perkin-Elmer 283 spectrophotometer as Nujol mulls between CsI plates.

**$W_2$(O-*i*-Pr)$_6$(py)$_2$($\mu$-$C_2H_2$).** In a Schlenk reaction flask, $W_2(O$-*i*-Pr$)_6$(py)$_2$ (0.80 g, 0.91 mmol) was dissolved in hexane/py (8 mL/0.5 mL). The dark red solution was frozen at −196 °C, and ethyne (0.91 mmol) was condensed into the flask by using a calibrated vacuum manifold. The reaction mixture was then stirred at room temperature for 4 h. The volume of the solution was reduced and the flask placed in the freezer at −15 °C for 18 h. A dark green crystalline solid was filtered from the solution and dried in vacuo (yield 0.69 g, 84%). Anal. Calcd for $W_2O_6N_2C_{30}H_{54}$: C, 39.75; H, 6.00; N, 3.09. Found: C, 39.48; H, 5.80; N, 3.05.

$^1$H NMR (−20 °C): $\delta$ (py, ortho) 9.25, m; $\delta$ (py, para) 6.87, t; $\delta$ (py, meta) 6.75, t; $\delta$ (OC*H*Me$_2$) 5.49 ($J_{HH}$ = 6 Hz) and 4.02 ($J_{HH}$ = 5 Hz), septets with intensity ratio 2:1, respectively; $\delta$ (OCH*Me*$_2$) 1.55 and 1.51 ($J_{HH}$ = 6 Hz), d, and 0.92 ($J_{HH}$ = 5 Hz), d; $\delta$ ($C_2H_2$) 8.63, s.

$^{13}$C NMR (−40 °C): $\delta$, ($C_2H_2$) 166.3, $J_{WC}$ = 41.6 Hz ($^1J_{CH} \simeq$ 192 Hz); $\delta$ (O*C*HMe$_2$) 80.3, 75.3; $\delta$ (OCH*Me*$_2$) 27.9 (br).

IR (cm$^{-1}$): 1601 m, 1571 vw, 1326 m, 1320 m, 1259 w, 1235 w, 1218 m, 1213 m, 1176 m, 1164 m, 1149 m, 1128 s, 1072 m, 1039 m, 1011 w, 998 m, 989 s, 962 m, 938 s, 845 m, 828 m, 758 m, 692 m, 629 m, 594 m, 566 w, 542 m, 460 m, 425 w, 346 vw, 312 m, 284 w.

**$W_2$(OCH$_2$-*t*-Bu)$_6$(py)$_2$($\mu$-$C_2$Me$_2$).** In a Schlenk reaction flask, $W_2(OCH_2$-*t*-Bu$)_6$(py)$_2$ (0.50 g, 0.48 mmol) was dissolved in hexane/py (6 mL/0.2 mL). The dark red solution was frozen at −196 °C, and 2-butyne (0.48 mmol) was added by using a calibrated vacuum manifold. The reaction mixture was stirred at room temperature for 2 h. During this time, the solution became dark blue and some precipitate formed on the walls of the flask. The volume of the solution was reduced to approximately 2 mL. Slight warming (40–50 °C) of the solution redissolved the precipitate. The solution stood at room temperature for 2 h and then was placed in a freezer at −15 °C for 1 h. A dark blue microcrystalline solid was collected by filtration and dried in vacuo (yield 0.41 g, 78%). Anal. Calcd for $W_2O_6N_2C_{44}H_{82}$: C, 47.92; H, 7.49; N, 2.54. Found: C, 47.68; H, 7.32; N, 2.46.

$^1$H NMR (21 °C): $\delta$ (py, ortho) 8.79 and 8.28, m; $\delta$ (py, para and meta) 7.00, 6.75, and 6.62, m; $\delta$ (OC*H*$_2$-*t*-Bu) 4.28 and 4.25, s, 4.22 and 4.03, d ($J_{HH}$ = 9.8 Hz) of an AB quartet, and 3.78 and 2.86, d ($J_{HH}$ = 10.7 Hz) of an AB quartet; $\delta$ (OCH$_2$C*Me*$_3$) 1.41, 1.17, 1.04, and 0.94, s with intensity ratio of 1:1:2:2, respectively; $\delta$ ($C_2$Me$_2$) 3.95, s.

IR (cm$^{-1}$): 1600 w, 1572 vw, 1258 vw, 1212 w, 1145 vw, 1092 s, 1071 s, 1039 m, 1022 s, 933 vw, 901 vw, 800 vw, 756 m, 695 m, 653 m, 646 m, 630 m, 620 m, 600 vw, 453 w, 405 w, 387 vw, 345 vw, 329 vw, 319 vw.

**$W_2$(O-*t*-Bu)$_6$(py)($\mu$-$C_2H_2$)·$^1/_2$py.** In a Schlenk reaction vessel, $W_2(O$-*t*-Bu$)_6$ (0.50 g, 0.62 mmol) was dissolved in hexane/py (15 mL/0.9 mL). The mixture was frozen at −196 °C, and ethyne (0.62 mmol) was condensed into the flask by using a calibrated vacuum manifold. The flask was transferred to an ice bath and allowed to warm to 0 °C. It was stirred at 0 °C for $^1/_2$ h. The solution turned from dark red to green during this time. The flask was then placed in a freezer at −15 °C. After 24 h, green microcrystals were collected by filtration and dried in vacuo. A second and third crop of crystals were collected (total yield 0.20 g, 34%). Anal. Calcd for $W_2O_6N_{1.5}C_{33.5}H_{63.5}$: C, 42.31; H, 6.73; N, 2.21. Found: C, 41.85; H, 6.65; N, 2.70.

$^1$H NMR (−80 °C): $\delta$ (py, ortho) 9.41 and 8.37, d; $\delta$ (py, para) 6.46, t; $\delta$ (py, meta) 6.07, two overlapping t; $\delta$ (py, free) 8.56, 6.83, and 6.55, m; $\delta$ (OC*Me*$_3$) 2.17, 1.98, 1.70, and 1.13, s with intensity ratio 1:1:2:2, respectively; $\delta$ ($C_2H_2$) 5.92, s.

$^{13}$C NMR (−40 °C): $\delta$ ($C_2H_2$) 120.1, $J_{WC}$ = 44.1 Hz ($J_{W_1C} \simeq J_{W_2C}$, $^1J_{CH} \simeq$ 184 Hz); $\delta$ (OCMe$_3$) 90.5, 81.8, 79.9, and 78.1; $\delta$ (OC*Me*$_3$) 34.0, 32.7, 32.1, and 29.7.

IR (cm$^{-1}$): 1603 m, 1570 vw, 1300 vw, 1222 m, 1171 s, 1067 w, 1040 w, 1022 m, 960 s, 905 m, 882 m, 780 m, 764 w, 702 w, 663 m, 628 w, 545 m, 490 w, 475 m, 372 m, 264 m.

**Labeled ethyne complexes** were prepared in an analogous manner employing either H$^{13}$C$^{13}$CH or DCCD.

**$W_2$(O-*t*-Bu)$_6$(py)($\mu$-*$C_2H_2$)·$^1/_2$py + $W_2$(O-*t*-Bu)$_6$(py)($\mu$-$C_2D_2$)·$^1/_2$py.** In a dry box, $W_2(O$-*t*-Bu$)_6$(py)($\mu$-*$C_2H_2$)·$^1/_2$py and the $\mu$-$C_2D_2$ analogue (35 mg of each) were placed in an NMR tube. Toluene-$d_8$ (0.5 mL) was added, the solution frozen in liquid $N_2$, and the tube sealed with a torch. The solution was warmed to room temperature (total time at room temperature, ca. 15–20 min) and then placed in the NMR probe cooled to −40 °C. $^{13}$C spectra were recorded in the usual manner.

**$W_2$(O-*t*-Bu)$_6$(py)($\mu$-*$C_2H_2$) + $C_2D_2$.** In a drybox, $W_2(O$-*t*-Bu$)_6$(py)($\mu$-*$C_2H_2$)·$^1/_2$py (35 mg, 0.037 mmol) was dissolved in toluene-$d_8$ (0.5 mL) in an NMR tube. The green solution was frozen and $C_2D_2$ (ca. 0.037 mmol) condensed into the tube by using a calibrated vacuum manifold. The tube was sealed with a torch and the sample allowed to warm to room temperature. As the tube warmed, the color darkened and acetylene polymer formation was observed. After 10 min at room temperature, the sample was placed in the NMR probe cooled to −40 °C and data were collected. Spectroscopic and chemical evidence for C–C bond formation by alkyne coupling for this and analogous compounds will be presented in a following paper.[9]

**$W_2$(O-*t*-Bu)$_6$($\mu$-*$C_2H_2$)(CO).** In a 15-mL two-neck round-bottomed flask was dissolved $W_2(O$-*t*-Bu$)_6$(py)(*$C_2H_2$)·$^1/_2$py (25 mg, 0.026 mmol) in hexane (2 mL). The green solution under $N_2$ (ca. 1 atm) was cooled to 0 °C. CO (0.026 mmol), drawn from a calibrated vacuum manifold with a 10-cm$^{-3}$ gas-tight syringe, was then added. The color of the solution darkened immediately. After the solution was stirred for 1 h at 0 °C and $^1/_2$ h at room temperature, the volatiles were removed in vacuo and the residue was redissolved in toluene-$d_8$. A small amount of insoluble material was present. Attempts to isolate a pure crystalline solid from preparative scale reactions carried out in a similar fashion have thus far been unsuccessful.

$^1$H NMR (21 °C): $\delta$ (OC*Me*$_3$) 1.31, 1.46, and 1.95, s with relative intensities 4:1:1, respectively (at −20 °C, the resonance at 1.31 ppm separates to two equally intense closely spaced singlets ($\Delta\nu$ = 1.44 Hz) due to a slight variation of the chemical shifts with temperature); $\delta$ ($^{12}C_2H_2$) 6.66, s.

$^{13}$C NMR (−40 °C): $\delta$ (OC*Me*$_3$): 32.6, 32.3, 31.2, 29.9; $\delta$ ($C_2H_2$) 125.5, $J_{W_1C}$ = 38 Hz and $J_{W_2C}$ = 25.1 Hz. The $^1$H and gate-decoupled $^{13}$C NMR spectra for the $^{13}$C-labeled complex each reveal half of the expected AA′XX′ spectrum in the ethyne region. Successful spectrum simulation gave $^1J_{CH}$ = 191.9 Hz, $^2J_{CH}$ = −1.7 Hz, $J_{CC}$ = 15.8 Hz, and $^3J_{HH}$ = 5.4 Hz. The relative signs of $^1J_{CH}$ and $^2J_{CH}$ are opposite, but undetermined. We chose $^2J_{CH}$ to be negative rather than $^1J_{CH}$. The relative signs of $J_{CC}$ and $^3J_{HH}$ are not known.

IR (cm$^{-1}$): $\nu_{CO}$ 1954 s.

**Crystallographic Studies.** General operating facilities and listings of programs have been given previously.[28] Crystal data for the three compounds studied in this work are given in Table IX.

**$W_2$(O-*i*-Pr)$_6$(py)$_2$($\mu$-$C_2H_2$).** The crystal used in the study was cleaved from a conglomerate and transferred to the goniostat by using standard inert-atmosphere handling techniques. The crystal was found to be isomorphous with $Mo_2(O$-*i*-Pr$)_6$(py)$_2$($\mu$-$C_2H_2$).[3]

The structure was solved by direct methods and Fourier techniques and refined by full-matrix least squares. All hydrogen atoms were located in a difference Fourier synthesis phased on the non-hydrogen atoms. Final least squares included isotropic thermal parameters for hydrogen atoms and anisotropic thermal parameters for all non-hydrogen atoms. A final difference Fourier synthesis revealed several large peaks (2.4, 2.1, and 1.8 e/Å$^3$) in the vicinity of the two tungsten atoms, and all other peaks were evenly distributed.

**$W_2$(OCH$_2$-*t*-Bu)$_6$(py)$_2$($\mu$-$C_2$Me$_2$).** A small equidimensional crystal was selected and transferred to the goniostat by using standard inert-

(29) During the course of these studies, Professor Schrock kindly informed us that he and his group believed that they had evidence for the formation of (*t*-BuO)$_3$W≡CH in the reactions between $W_2(O$-*t*-Bu$)_6$ and terminal alkynes, specifically 1-hexyne. We subsequently found that when 1 equiv of 1-hexyne is added to a toluene-$d_8$ solution of $W_2(O$-*t*-Bu$)_6$ + 1.5py at room temperature, an immediate reaction occurs, yielding a green solution. The $^1$H NMR spectrum of this solution at −60 °C showed the characteristic signals assignable to $W_2(O$-*t*-Bu$)_6$(py)($\mu$-$C_2H_2$) in addition to the signal we have assigned to (*t*-BuO)$_3$W≡CH and other resonances probably arising from (*t*-BuO)$_3$W≡C(CH$_2$)$_3$CH$_3$. The relative ratio of the signals assignable to the $W_2$($\mu$-$C_2H_2$) and W≡CH moieties was ca. 10:1. These results are understandable in terms of the combined reactions 1 and 3.

**Table IX.** Summary of Crystallographic Data[a]

| | I | II | III |
|---|---|---|---|
| fw | 908.48 | 1102.84 | 951.05 |
| space group | $P2_1/a$ | $C2/c$ | $P\bar{1}$ |
| $a$, Å | 19.061 (11) | 37.822 (21) | 17.399 (5) |
| $b$, Å | 15.674 (7) | 12.207 (5) | 11.336 (3) |
| $c$, Å | 12.234 (5) | 22.163 (9) | 11.216 (3) |
| $\alpha$, deg | | | 71.53 (1) |
| $\beta$, deg | 108.08 (1) | 101.01 (2) | 113.72 (1) |
| $\gamma$, deg | | | 98.90 (2) |
| $Z$ | 4 | 8 | 2 |
| $V$, Å$^3$ | 3474.46 | 10044.64 | 1919.96 |
| $d_{calcd}$, g/cm$^{-3}$ | 1.737 | 1.459 | 1.714 |
| cryst size, mm | 0.08 × 0.08 × 0.07 | 0.15 × 0.15 × 0.15 | 0.08 × 0.08 × 0.08 |
| cryst color | red | black | black |
| radiatn | | Mo K$\alpha$ ($\lambda$ = 0.71069 Å), graphite monochromator | |
| linear abs coeff, cm$^{-1}$ | 67.976 | 47.158 | 61.579 |
| transmissn factors | 0.609–0.665 | no abs corr | no abs corr |
| temp, °C | −165 | −160 | −160 |
| instrument | | Picker four-circle diffractometer locally modified and interfaced | |
| detector aperture | | 3.0 mm wide × 4.0 mm high, 22.5 cm from crystal | |
| sample to source distance, cm | | 23.5 | |
| takeoff angle, deg | 2.0 | 2.0 | 2.0 |
| scan speed, deg/min | 4.0 | 6.0 | 4.0 |
| scan width, deg | 1.8 + 0.692 tan $\theta$ | 1.7 + 0.692 tan $\theta$ | 1.7 + 0.692 tan $\theta$ |
| bkgd counts, s, at each end of scan | 5 | 4 | 10 |
| 2$\theta$ range, deg | 6–50 | 6–45 | 6–45 |
| data collected | 7351 total | 7811 total | 5299 total |
| unique data | 6155 | 6602 | 5029 |
| unique data with $F_o > 2.33\sigma(F_o)$ | 4709 | 5548 | 4064 |
| $R(F)$ | 0.056 | 0.052 | 0.040 |
| $R_w(F)$ | 0.049 | 0.051 | 0.040 |
| goodness of fit | 1.072 | 1.311 | 1.059 |
| largest $\Delta/\sigma$ | 0.05 | 0.05 | 0.05 |

[a] I, $W_2(O\text{-}i\text{-}Pr)_6(py)_2(\mu\text{-}C_2H_2)$; II, $W_2(OCH_2\text{-}t\text{-}Bu)_6(py)_2(\mu\text{-}C_2Me_2)$; III, $W_2(O\text{-}t\text{-}Bu)_6(py)(\mu\text{-}C_2H_2)\cdot{}^1/_2py$.

atmosphere handling procedures. A systematic search of a limited hemisphere of reciprocal space yielded a set of reflections that possessed monoclinic symmetry and exhibited systematic extinctions consistent with the space group $C2/c$.

The structure was solved by standard heavy-atom methods. The two W atoms were located by means of a Patterson function, and standard Fourier techniques located the remaining atoms. A difference Fourier computed after the initial refinements showed the positions of most of the hydrogen atoms. The hydrogen atoms were introduced in calculated positions in the subsequent cycles of refinement. All non-hydrogen atoms are refined by using anisotropic thermal parameters. The hydrogen atom positions were recomputed after each round of refinements, but their positions were not varied due to the large number of parameters. No absorption corrections were deemed necessary. The refinements were carried out by using full-matrix least-squares techniques, using 5647 reflections having $F$ greater than $3\sigma(F)$.

The final difference Fourier was essentially featureless, except for several peaks in the vicinity of the W atoms.

**$W_2$(O-t-Bu)$_6$(py)($\mu$-$C_2H_2$).** A suitable crystal was cleaved from a larger sample and transferred to the goniostat by using standard inert-atmosphere techniques. A systematic search of a limited hemisphere of reciprocal space revealed no systematic absences or symmetry, suggesting a triclinic space group.

The structure was solved by Patterson and Fourier technique and refined by full-matrix least squares. Hydrogen atoms were clearly visible in a difference Fourier phased on the non-hydrogen atoms and were refined isotropically in the final cycles of refinement. It was at this stage that problems were encountered. One of the hydrogens associated with the HCCH group lies out of the plane bisecting the W–W bond, and further, the two carbon atoms are more anisotropic than one would expect, based on the apparent quality of the data. An attempt to correct the data for absorption did not improve the thermal parameters (the minimum and maximum transmission only varied from 0.79 to 0.83).

For this reason, a second crystal, obtained from a different reaction mixture, was examined. A small crystal with well-defined faces was chosen. The data were recollected, and an absorption correction was made. Unfortunately, the thermal parameters for the HCCH ligand were not significantly better, and further, several of the hydrogens would not converge properly, including both of those associated with the HCCH. The distances and angles involving the non-hydrogen atoms were essentially identical with those obtained for crystal I.

The positions of the hydrogen atoms, though qualitatively correct, are poorly determined, as is often the case with heavy-atom structures. Therefore, no chemical significance is attached to the apparent twist in the bridging H–C–C–H group.

**Acknowledgment.** We thank the donors of the Petroleum Research Fund, administered by the American Chemical Society, the Department of Energy, Office of Basic Chemical Sciences Division, and the Wrubel Computing Center for support of this work. We are also grateful to the National Science Foundation for Instrument Grant No. CHE 81-05004.

**Registry No.** IV, 91389-16-1; $W_2(O\text{-}t\text{-}Bu)_6(py)(\mu\text{-}{}^*C_2H_2)$, 91389-15-0; $W_2(O\text{-}i\text{-}Pr)_6(py)(\mu\text{-}C_2H_2)$, 82281-73-0; $W_2(OCH_2\text{-}t\text{-}Bu)_6(py)_2(\mu\text{-}C_2Me_2)$, 87684-89-7; $W_2(O\text{-}t\text{-}Bu)_6(py)(\mu\text{-}C_2H_2)\cdot{}^1/_2py$, 91463-88-6; $W_2(O\text{-}t\text{-}Bu)_6(py)(\mu\text{-}C_2H_2)$, 87667-98-9; $W_2(O\text{-}t\text{-}Bu)_6(py)(\mu\text{-}HCCD)$, 91389-17-2; $W_2(O\text{-}i\text{-}Pr)_6(py)_2$, 70178-75-5; $W_2(OCH_2\text{-}t\text{-}Bu)_6(py)_2$, 88608-50-8; $W_2(O\text{-}t\text{-}Bu)_6$, 57125-20-9; $W_2(O\text{-}t\text{-}Bu)_6(py)(\mu\text{-}C_2D_2)$, 91389-18-3; $W_2(O\text{-}i\text{-}Pr)_6(py)_2(\mu\text{-}C_2D_2)$, 91389-19-4; $(t\text{-}BuO)_3W{\equiv}CH$, 91389-20-7; $(t\text{-}BuO)_3W{\equiv}C(CH_2)_3CH_3$, 91389-21-8.

**Supplementary Material Available:** Complete listings of bond lengths and bond angles, anisotropic thermal parameters, and structure factor amplitudes (28 pages). Ordering information is given on any current masthead page. The complete structural reports are available from the Indiana University Chemistry Library, in microfiche form only. Request MSC Report No. 83019, 82101, and 82009 for $W_2(O\text{-}t\text{-}Bu)_6(py)(C_2H_2)\cdot{}^1/_2py$, $W_2(OCH_2\text{-}t\text{-}Bu)_6(py)_2(C_2Me_2)$, and $W_2(O\text{-}i\text{-}Pr)_6(py)_2(C_2H_2)$, respectively.

(30) **Note Added in Proof:** $^1J_{^{13}C-^{13}C}$ = 9.2 Hz for the ring carbons in tetra-*tert*-butyltetrahedrane has recently been reported: Loerzer, T.; Machinek, R.; Lüttke, W.; Franz, L. H.; Malsch, K.-D.; Maier, G. *Angew. Chem., Int. Ed. Engl.* **1983**, *22*, 878.